

**THE UNIVERSITY OF WESTERN ONTARIO
DEPARTMENT OF CIVIL AND
ENVIRONMENTAL ENGINEERING**

Water Resources Research Report

**Assessment of climatic vulnerability in the Upper
Thames River basin: Downscaling with LARS-WG**

By:

**Sarah E. Irwin
Rubaiya Sarwar
Leanna M. King
and
Slobodan P. Simonovic**

**Report No: 081
Date: April 2012**

**ISSN: (print) 1913-3200; (online) 1913-3219;
ISBN: (print) 978-0-7714-2964-4; (online) 978-0-7714-2965-1;**



Assessment of Climatic Vulnerability in the Upper Thames River Basin:

Downscaling with LARS-WG

Sarah E. Irwin

Rubaiya Sarwar

Leanna M. King

Slobodan P. Simonovic



Department of Civil and Environmental Engineering

The University of Western Ontario

London, Ontario, Canada

February 2010

Executive Summary

As a result of human induced greenhouse gas emissions the IPCC expects the average global temperature to rise in future years. It is important to understand how such change to the earth's climate system will affect future precipitation amounts and frequencies as these variables are directly related to rising water levels and potential flooding events. Currently hydrologic models use historical daily or hourly precipitation as input to measure stream flows and corresponding water levels. However, it is becoming that the assumption of a stationary climate is no longer valid. Atmospheric Ocean-coupled Global Climate Models are the most credible tool for projecting future climate as they reliably produce monthly climate at a global scale. To predict future extreme hydrologic events AOGCM data is used as an input to hydrologic models. However, such data cannot be used directly as hydrologic models require local-scale daily precipitation as input. Therefore, AOGCM outputs must be manipulated to the appropriate spatial and temporal scale using statistical downscaling tools such as LARS-WG, SDSM, and KnnCAD.

This study includes a detailed analysis of the stochastic weather generator LARS-WG as well as a more general comparative analysis between LARS-WG and the two other models SDSM and KnnCAD (Version 3). A 27-year historical dataset (1979-2005) from the London International Airport station in the Upper Thames River Basin is used as an input for the downscaling models, which simulate 324 years of synthetic daily climate variables. All models undergo a performance evaluation where their ability to reproduce observed weather statistics is tested. Simulation of future climate variables is done through the modification of historical datasets using change factors from the difference in current and future AOGCM output.

For LARS-WG's performance evaluation, it is evident that total monthly precipitation, total number of wet days, and minimum and maximum temperatures are well reproduced as the observed medians lie within the inter-quartile range of simulated weather for all variables in each month. In fact

many of the observed medians coincide with the simulated medians, particularly for total monthly precipitation results. As for wet spell frequencies there is some discrepancy as to whether one or two-day wet spell lengths occur most often, otherwise they are also simulated well. Overall, LARS-WG successfully reproduces observed weather statistics.

Next LARS-WG's ability to simulate future weather variables including total monthly precipitation, total monthly number of wet days and minimum and maximum temperatures is tested. Fifteen different AOGCM and emission scenario combinations are used to modify the historical datasets. For total monthly precipitation, the majority of models agree that precipitation will increase between the months of January to May and October to December, while most models project a decrease in precipitation between June to September. The magnitudes of change in precipitation increase significantly between 2020 and 2080 periods, and models become more agreeable with time. The change in total number of wet days between baseline and future time periods varies significantly between months, however model projections are agreeable within each month, otherwise there are no obvious trends. All results for minimum and maximum temperatures are projected to increase in the 2020 time period, and further increase in the 2080s. AOGCMs driven by the A1B scenario tend to project the greatest increase in temperature.

The performance evaluation for the comparative analysis takes into account absolute maximum and minimum temperatures, total monthly precipitation, and the mean and standard deviation of daily precipitation. KnnCAD best reproduces absolute minimum and maximum temperatures as all monthly historical and simulated maximum temperature values coincide, and there is only a small discrepancy in minimum temperature results between October to December. LARS-WG and SDSM successfully reproduce temperatures as well. All downscaling models simulate precipitation amounts quite well, however LARS-WG and KnnCAD are far superior at reproducing precipitation statistics including the mean and standard deviation. There is no correlation between datasets for SDSM's projection of mean daily precipitation.

Future daily precipitation amount is the only variable involved in the comparative analysis of the three downscaling models. It is evident that each season projects fairly different results, however there are distinct patterns within the individual seasons. In addition, LARS-WG and KnnCAD tend to project similar outcomes year round. SDSM projects the greatest increase in precipitation for the winter season, while LARS-WG and KnnCAD results are less significant. The opposite is true for the spring season as LARS-WG and KnnCAD project the greatest increase in precipitation, and the majority of SDSM results project a decrease in precipitation. In the summer season LARS-WG results are variable and the majority of KnnCAD results predict a decrease in precipitation, while all SDSM simulations consistently project the greatest increase in precipitation. Finally in the fall season, LARS-WG and KnnCAD project similar results that provide the greatest magnitude of precipitation increase.

Table of Contents

1. Introduction.....	1
2. Literature Review.....	3
3. Study Area	9
4. Data.....	11
5. Methodology.....	15
5.1 The Validation Procedure	15
5.2 Development & Application of Change Factors.....	15
5.3 LARS-WG	17
5.4 SDSM.....	18
5.5 KnnCAD	20
6. Results.....	21
6.1 Validation and Performance Evaluation	22
6.2 Generation of Future Climate Variables	28
6.2.1 Total Monthly Precipitation	28
6.2.2 Total Monthly Number of Wet Days	33
6.2.3 Temperature	37
7. Comparison Between LARS-WG, SDSM, KnnCAD.....	43
6.1 Comparative Performance Evaluation of LARS-WG, SDSM, KnnCAD.....	43
6.2 Comparative Generation of Future Daily PPT by LARS-WG, SDSM, KnnCAD ...	46
8. Conclusions.....	51
References.....	54
Appendix A: Atmosphere-Ocean General Circulation Model Data Description	59
Appendix B: SRES Emission Scenarios:.....	61
Appendix C: AOGCM Figures for 2050s	63

List of Tables

Table 1: Weather data used for model input

Table 2: List of AOGCM models and emissions scenarios used

Table 3: Percent change results for total seasonal precipitation amounts for LARS-WG, SDSM, and KnnCAD; 2050s

List of Figures

Figure 1: Schematic location map of Upper Thames River Basin

Figure 2: Validation results for total monthly precipitation using 541, 1223, 2741, and 4409 random seeds

Figure 3: LARS-WG performance evaluation results for total monthly precipitation

Figure 4: LARS-WG performance evaluation results for total number of wet days

Figure 5: LARS-WG Performance evaluation results for minimum temperature

Figure 6: LARS-WG performance evaluation results for maximum temperature

Figure 7: LARS-WG fair performance evaluation results for wet spell lengths in July

Figure 8: LARS-WG successful performance evaluation results for wet spell lengths in September.

Figure 9: Percent change in total monthly precipitation, 2020s

Figure 10: Percent change in total monthly precipitation, 2080s

Figure 11: Percent change in total monthly number of wet days, 2020s

Figure 12: Percent change in total monthly number of wet days, 2080s

Figure 13: AOGCM predictions for maximum temperature, 2020s. Emission scenarios A1B, A2, B1 from top to bottom

Figure 14: AOGCM predictions for minimum temperature, 2020s. Emission scenarios A1B, A2, B1 from top to bottom

Figure 15: AOGCM predictions for maximum temperature, 2080s. Emission scenarios A1B, A2, B1 from top to bottom

Figure 16: AOGCM predictions for minimum temperature, 2080s. Emission scenarios A1B, A2, B1 from top to bottom

Figure 17: Comparative performance evaluation results for LARS-WG, SDSM, and KnnCAD

Figure 18: Percent change in total monthly precipitation, 2050s

Figure 19: Percent change in total monthly number of wet days, 2050s

Figure 20: AOGCM predictions for maximum temperature, 2050s. Emissions scenarios A1B, A2, B1 from top to bottom

Figure 21: AOGCM predictions for minimum temperature, 2050s. Emissions scenarios A1B, A2, B1 from top to bottom

1. INTRODUCTION

It is suspected that human-induced climate change has the potential to increase the frequency and severity of extreme weather events such as heat waves, floods and droughts. Climate change is defined as a difference in the mean and variability of weather variables over a significant period of time, typically several decades. The driving forces of climate change may be natural, such as ocean oscillations and solar radiation, or human induced greenhouse gases that alter the composition of the atmosphere. Since the industrial revolution of the 18th and 19th centuries humans have increased their reliance on fossil fuels for transportation, energy production and heating processes which emit significant amounts of carbon dioxide into the atmosphere. Other processes such as deforestation and agricultural activities also contribute to the rising greenhouse gas concentrations. As a result of these activities the IPCC has predicted that the mean global temperature could increase by 3 degrees Celcius by 2080 (IPCC, 2007).

Change to one component of the earth's climate system will disrupt the balance in another. The climate system is composed of five interactive components including the atmosphere, hydrosphere, cryosphere, lithosphere, and biosphere. It is expected that an increase in the earth's average temperature will cause an imbalance in the hydrologic cycle resulting in a greater number of extreme precipitation events (IPCC, 2007). As such, it is important to perform climate change impact assessments to understand how these future extremes will affect our society, economy and the environment. This can be done through hydrologic modeling. Daily precipitation from historical records is typically used as an input to hydrologic models which predict resultant stream flow rates and corresponding water levels in reservoirs and other water bodies. These models are essential to water resources management and the development of prevention measures for future flooding events. However, it is becoming that historical

precipitation records are no longer suitable to predict future events as the assumption of a stationary climate is no longer valid. Consequently, it is important to develop a reliable method of predicting future climate variables for the use of hydrologic impact analyses.

Current weather is measured and collected at weather stations with historical records easily accessible on databases, but future weather conditions must be simulated. Global Climate Models (GCM's) are the most credible tool for producing future climate variables in response to increased greenhouse gas concentrations (Dibike, 2004). Atmosphere Ocean-coupled Global Climate Models (AOGCMs) are a branch of GCMs that provide a three-dimensional representation of the Earth-Atmosphere-Ocean climate system (CCCSN, 2011). Models of the oceans, atmosphere, sea-ice, land surface, global carbon cycle, and aerosols are linked together to simulate system changes, (CSIRO, 2011). They are driven by emissions scenarios that provide plausible representations of how the future will unfold with respect to the major influences of greenhouse gas emissions such as population growth, economic development, technical advancements, resource use and pollution control; refer to Appendix B (IPCC, 2007).

AOGCMs can accurately represent monthly averages of global climate data, however hydrologic models require a daily time-series of local weather variables as input. Computational power is the AOGCMs limiting factor. They must compromise spatial resolution for time to run the model, and as a result their resolution is too coarse to adequately represent watershed level processes such as precipitation (Semenov, 1997). In order to use global climate data as input to hydrologic models, it must be manipulated to the appropriate spatial and temporal scales using downscaling techniques.

There are two main types of downscaling techniques: dynamic downscaling and statistical downscaling (Brisette, 2006). In this report three statistical downscaling tools are analysed and compared. Each model has a unique structure and uses different statistical methods to simulate daily climate variables. This study will analyse a range of outputs produced by the various models to encompass all plausible weather extremes. It is necessary to understand the magnitude of future climate extremes to effectively manage water resources and prevent severe events such as flooding or drought from damaging infrastructure and endangering the population.

2. LITERATURE REVIEW

There are several techniques available for downscaling global climate data to an appropriate spatial and temporal scale. Each method has its own benefits and limitations, and improvements are continuously being made to their structures. A single tool has not been identified as the best option, so multiple approaches must be considered for simulating a daily time-series of present or future climate data.

Dynamic downscaling uses a Regional Climate Model (RCM) nested within an AOGCM to simulate high resolution climate data that is more reliable than direct AOGCM output. On average an RCM has a 40x40 km² resolution which is a great improvement to the approximate 250x250 km² resolution of the AOGCM, however its grid size is still much larger than many watersheds (Brisette, 2006). It would be inaccurate to apply RCM output to such small watersheds for the same reasons that global climate data should not be used directly at local-scales. A major disadvantage to this method is the RCM's strong dependence on biased input from the AOGCM it is nested within. In addition, it is a computationally demanding process which limits the number of simulations that can be processed in a timely fashion (CCCSN, 2011). Because of this, RCMs cannot easily cover the entire scope of plausible future climate outcomes.

The alternative approach is statistical downscaling, which includes regression downscaling or the use of a stochastic weather generator. Both methods assume a statistical relationship between local and large-scale weather data, (Corte-Real, 1999). Regression downscaling estimates local variables (predictands) from large-scale AOGCM outputs (predictors) using regression equations and transfer functions. The user must first select the most relevant predictor variables. This is done by determining which large-scale variables produce the strongest linear correlation with the required local-scale variables through the development and analysis of scatter plots. To downscale global climate data the selected predictor variables are then used as inputs to the regression model and resultant future daily weather is simulated. Statistical Down-Scaling Model (SDSM) is a well-recognized regression model developed by Wilby *et al.* (2002). In a study on the Chute-du-Diable Basin in Quebec, it was discovered that SDSM produced a good relationship between observed and simulated outputs for the mean and variability of daily precipitation, as well as average monthly dry spell lengths. However average monthly wet spell lengths were consistently underestimated (Dibike, 2004). This is a major flaw as persistent precipitation events are a primary cause of flooding. Another disadvantage of all regression models is their inability to simulate multi-site weather variables and preserve the spatial correlation that is present in the observed weather (Semenov, 1997; Apipattanavis *et al.*, 2007). Also because of the assumed relationship between AOGCM output and site-specific observed data, models are not easily transferrable between different sites (Wilby, 2004).

Stochastic weather generators use historical datasets as input and produce a synthetic time-series that is statistically similar to the observed climate, (Dibike, 2004). They were originally developed for hydrologic or agricultural risk assessments, and extending weather simulations to unobserved locations through spatial interpolation techniques. More recently

weather generators have been used in climate change studies as a means of downscaling future global climate data (Semenov 1997; Wilks and Wilby, 1999). Downscaling is achieved by applying AOGCM change factors to the observed weather data, then running the modified datasets through the weather generator to produce a daily time-series of future climate variables, (Diaz-Nieto, 2005; Wilby, 2002). Weather generators are computationally inexpensive and capable of simulating time-series of infinite lengths, which is beneficial for a risk analysis of extreme weather events.

There are three main groups of weather generators and multiple models within each group. Parametric weather generators are the most primitive models. They use a first order, two-state Markov chain to simulate precipitation occurrence. Variables such as precipitation amount, temperature and solar radiation are then selected from simple probability distributions that are conditional upon the precipitation status of that day. For example, solar radiation is related to the amount of cloud cover so there are separate radiation distributions for wet and dry days. This procedure preserves the correlation between variables. Precipitation is modeled using a two-parameter gamma distribution, while normal distributions are used for all other variables (Hanson and Johnson, 1998; Soltani, 2003; Kuchar, 2004; Dibikey, 2004). There are various advantages and disadvantages to the standard distributions used in parametric weather generators. They characteristically have a smoothing effect on input parameters, and as a result smooth over observed errors. However, this effect may also smooth over extreme values so they are not accurately represented in the generated output (Mason, 2004). Appropriate distributions are assumed to fit each variable which can be a subjective process. In addition, the selection of a suitable probability distribution is site-specific, therefore these models are not easily transferrable between sites in different climatic regions (Rajagopalan, 1997; Sharif and Burn,

2007). The first such parametric model is WGEN, which is the traditional weather generator developed by Richardson (1981). Various other parametric models have been developed as extensions of WGEN including WXGEN which takes into account new variables such as the non-normal distributions of wind speed and relative humidity (Nicks *et al.*, 1990). Generation of Weather Elements for Multiple Applications (GEM) also incorporates wind speed and dew point from which relative humidity can be derived, (Hanson and Johnson, 1998). Several multi-site parametric models have been developed that preserve the spatial correlation of observed weather variables, (Hughes and Guttrop 1994; Wilks 1998). The main short-coming of parametric models is their inability to produce wet and dry spell lengths due to the structure of the first order Markov chain. It determines the precipitation status of the next day based on the current day's status, and the previous day's weather is not considered. Consequently, it does not reproduce the temporal correlation that is prominent in the historical datasets (Sharif and Burn, 2007).

The serial approach to weather generation came about in response to the limitations of the parametric weather generator such as underestimated spell lengths. The first serial-type weather generator was developed by Rascko *et al.* (1991). Instead of using a Markov chain to simulate precipitation occurrence day by day, it selects entire wet and dry spell lengths from predetermined probability distributions. Semenov and Barrow (1997) extended this method by replacing the predetermined distributions with semi-empirical distributions created through the analysis of historical records. Their semi-parametric model known as LARS-WG, has proven to reproduce wet and dry spell frequencies quite well during the validation process (CCIS, 2007; Dibike, 2004). Approximate standard distributions were also replaced with semi-empirical distributions for climate intensity variables. Again, weather parameter input is analyzed to produce semi-empirical distributions that are flexible enough to fit any distributional shape. As

such, errors from the input parameters may be reproduced, but these models are better at capturing extreme precipitation intensities. Also, since site-specific assumptions are not made between variables and a distribution of best-fit, the model is easily transferrable between sites. As with parametric models, variables are conditioned upon the precipitation status of the day and selected from separate wet or dry semi-empirical distributions accordingly (Semenov *et al.*, 1997, 1999). Although great progress has been made from the traditional parametric weather generator, LARS-WG has its own shortcomings. Semenov and Barrow (1997) developed LARS-WG for the purpose of agricultural risk assessments, so its output was intended to be used as input to crop growth models that require a daily time-series of climate data at a single site. As a result, LARS-WG is not programmed for multi-site generation which is preferred for hydrologic risk assessments. In many cases hydrologic modeling requires climate data over extensive areas and without multi-site generation the spatial correlation in the observed weather is lost. Through a comparative study, Dibike (2004) concluded that downscaling with LARS-WG produced an increasing trend in mean monthly minimum and maximum temperatures, and a slight decrease in temperature variability for most months. Conversely, results suggested there was no significant change in mean monthly precipitation or wet and dry spell lengths. Such results are not desirable when estimating precipitation extremes.

Non-parametric weather generators are another category of statistical downscaling models, and of this type the K-nearest-neighbour (K-NN) algorithms are the most promising, (Apipatanavis, 2007). Developed by Young (1994), the model simultaneously samples and replaces weather variables from a window of time in the historical datasets. Instead of simulating variables individually, an entire day's weather is selected at once. This characteristic allows for the preservation of multivariate correlations that exist in the observed data. Several extensions of

the original K-NN model have been made. For example, Brandsma and Buishand (1998) used a K-NN model to simulate precipitation and temperature at various single sites in the Rhine Basin, and further extended their model to perform multi-site simulations (2001). Another advancement was made by Yates *et al.* (2003) who developed a K-NN model capable of generating climate change scenarios. While it is an improvement from many of the parametric models, the K-NN weather generator has some drawbacks. Apipatanavis (2007) used such model in a study to discover an underestimation of the fraction of dry months. K-NN weather generators tend to underestimate persistent precipitation events due to their simulation procedure. Precipitation is an intermittent variable and its occurrence should be simulated independently to maintain a temporal correlation. Since a day's weather is selected based on the weighted average of an entire suite of variables (temperature, precipitation, humidity, solar radiation), the temporal correlation of precipitation is not well reproduced and prolonged spell lengths have a tendency to be underestimated. In response to this study, Apipatanavis (2007) developed a modified K-NN model that uses a Markov chain to determine the daily precipitation status from which other variables are conditioned upon. Results for average spell lengths were improved but maximum wet and dry spell lengths were still not accurately reproduced. This is likely due to the limitations of the Markov chain as it cannot take more than one day of historical weather into account. Another major disadvantage of the traditional K-NN model is its inability to produce unprecedented values as the input weather variables are merely reshuffled. Sharif and Burn (2006) addressed this issue by adding a random component to the historical input, known as perturbation. As a result of this process the model is capable of producing temperature and precipitation variables that differ from the observed datasets, which is important for the simulation of hydrologic extremes. Through a comparative study in the Upper Thames River

watershed in south-western Ontario, Sharif and Burn (2006) determined that the modified K-NN model is capable of simulating unprecedented yet realistic results. Also, future climate results are more extreme than with previous models.

Each downscaling technique has its own biases due to their different statistical methods and assumptions. As a result every model produces distinct outcomes and uncertainties, even when the same inputs are used. This report compares a suite of AOGCM outputs downscaled by three unique weather generators: SDSM, LARS-WG, and KnnCAD. The various combinations of AOGCMs and downscaling models will provide a wide range of future weather data for the purpose of predicting climate extremes.

3. STUDY AREA

This study takes place in the Upper Thames River watershed (**Figure 1**) which is situated in south-western Ontario, Canada. It covers 3482 km² of land that is mainly rural except for large urban centres of London, Stratford, Woodstock, St. Mary's, and Mitchell. Streams and creeks collect run-off from the entire catchment area and flow into a major waterway known as the Thames River. The river spans 273 kilometres from Tavistock to the mouth of Lake St. Clair, and is composed of two major branches. The north branch flows southward through Mitchell, St. Mary's, and London. The east branch flows westward through Woodstock, Ingersoll, and into London where it meets the north branch at the Forks in downtown London. From there the river flows as a single channel out of the west end of the city and eventually drains into Lake St. Clair (Upper Thames, 2011; Prodanovic and Simonovic 2007).

The Upper Thames River Basin was once covered by a dense deciduous forest, but today much of that forest has been cleared for urban and agricultural growth. In fact, agriculture

accounts for 80 percent of the watershed's land use because of the area's silty, nutrient-rich soil, (Prodanovic and Simonovic, 2007). Such changes to the natural landscape increase the potential for flooding events. Prior to land development, swamps and forests naturally moderated water levels in the Thames and its tributaries. Rainfall was retained and slowly released into the river as surface or groundwater. Urban and agricultural developments have introduced impervious land surfaces and sewer systems that carry storm water to the river much more quickly, resulting in uncontrolled, rapidly rising water levels (Thames Topics, 1999).

The Thames River has a history of flooding events, the most severe of which occurred in April 1937. The watershed experienced thirteen centimetres of rainfall over a six day period, just after the water levels had risen due to the spring melt. This extreme precipitation event led to the highest flood levels ever recorded in the area, and consequently over 1,100 homes and businesses were damaged. In response to this natural disaster the provincial government implemented the Conservation Authority Act of 1946, and the following year the Upper Thames River Conservation Authority (UTRCA) was established. As part of their mandate the UTRCA agreed to protect people and properties from flooding. So far they have been quite successful due to the implementation of three dams along the river including Fanshawe (completed in 1953), Wildwood (completed in 1965), and Pittock (completed in 1967), (Thames Topics, 1999).

The IPCC suggests that northern countries, including south-western Ontario Canada, will experience more frequent and extreme precipitation events as a response to climate change. It is important to ensure water management methods and flood control structures are sufficient to withstand the severity of future events. More work is required to properly assess the vulnerability of extreme climate on the Upper Thames River Basin (IPCC, 2007; Solaiman and Simonovic, 2010).

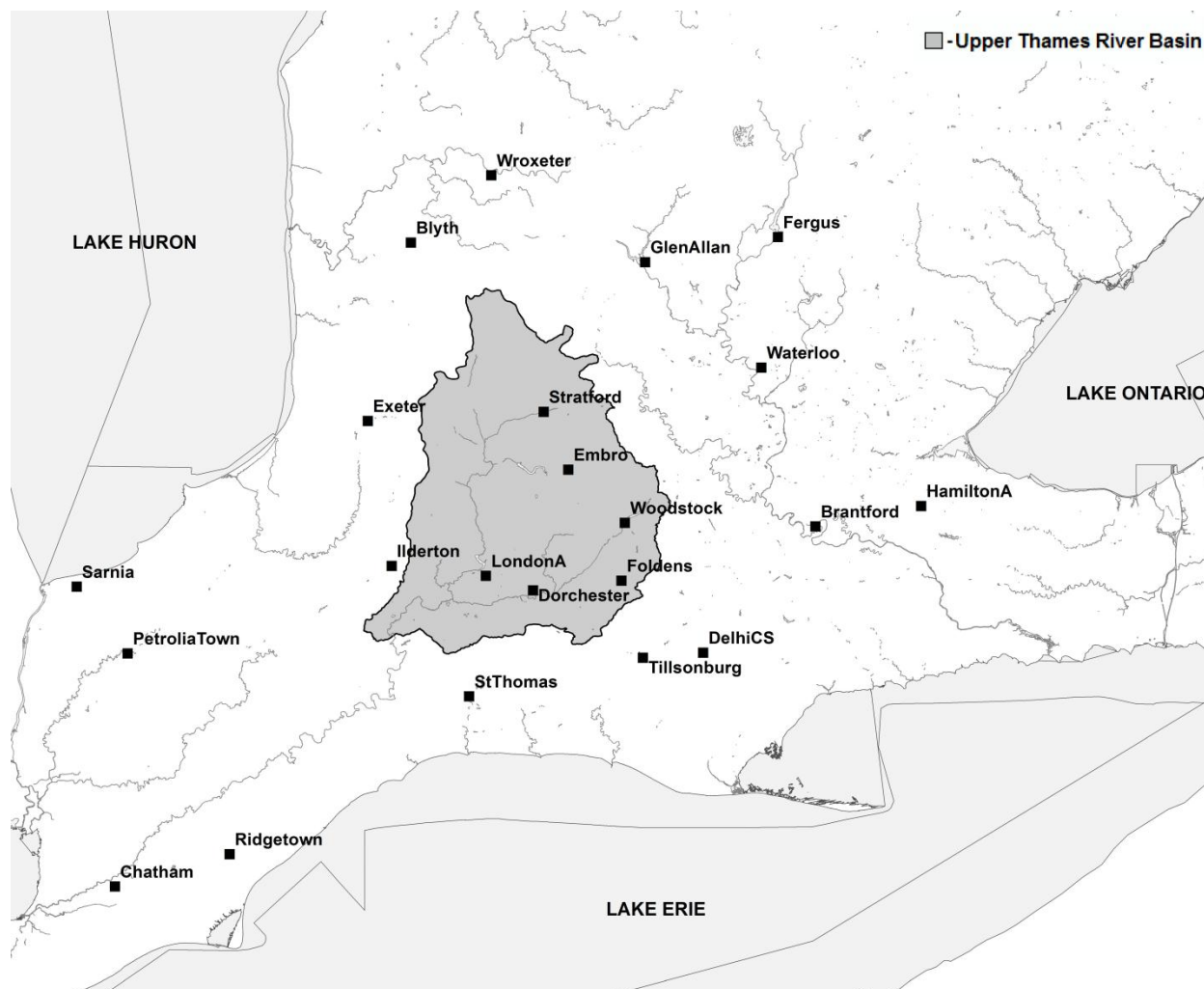


Figure 1: Schematic location map of the Upper Thames River watershed (Statistics Canada, 2006a; 2006b)

4. DATA

Historical records of climate data were collected from several sources for the London Airport station in the Upper Thames River Basin. Precipitation and temperature records were obtained from the Environment Canada website. Humidity, wind speeds, mean sea level pressure, and other meteorological variables that were not made available by Environment Canada, were acquired from the North American Regional Reanalysis (NARR) database. **Table 1** provides a description of each of the weather variables as well as their source.

In this study, outputs from LARS-WG and SDSM are compared to KnnCAD output available in *Assessment of Climatic Vulnerability in the Upper Thames River Basin: Part 2* by King *et al.* (2010). For an accurate comparison it is important to ensure input parameters are consistent for all three weather generators, thus these resources are the same as those used in the King *et al.* (2010) study.

The Environment Canada website has a Canadian Daily Climate Data program that provides publicly accessible historical climate data for specified stations and time periods. Its interface allows the user to select the site, time period, and interval (hourly, daily, monthly) for which the data is presented. For this study daily precipitation, minimum temperature, and maximum temperature are obtained for the 27 year period from 1979-2005. This time period is selected because it contains complete datasets for all stations used in *Assessment of Climatic Vulnerability in the Upper Thames River Basin: Part 2* by King *et al.* (2010).

In order to include a variety of weather variables for the KnnCAD and SDSM models, NARR data is also employed in this study. The goal of NARR is to create a long-term database of consistent climate data for all of North America. It uses the regional Eta model which simulates high resolution weather variables that are superior to NCEP/NCAR Global Reanalysis output. Since the high resolution grid size is not sufficient to cover the planet's entire surface area, Global Reanalysis 2 supplies its boundary conditions. The Eta model has a spatial resolution of 32x32 km² and 45 atmospheric layers in the vertical. Temporally, it is capable of simulating climate variables at 3 hour intervals or 8 times daily, (NARR, 2007). It assimilates a suite of non-standard variables including wind speeds, humidity, and mean sea level pressure that are extracted and used as an input for the SDSM and KnnCAD weather generators. For this study the NARR gridded weather data are obtained on request from the National Oceanic and

Atmospheric Administration (NOAA), and interpolated for the London Airport station in the Upper Thames River Basin.

AOGCM outputs are used to create climate change scenario files which contain the change factors used to modify the historical datasets for the generation of the future climate variables. The AOGCM outputs may be accessed through the Canadian Climate Change Scenario Network (CCCSN) website. The website has a user friendly interface where one may select an AOGCM driven by one of three emissions scenarios, a climate variable to be simulated, and the time period of consideration. The available AOGCMs or RCMs are those published in the IPCC's assessment reports, the most recent of which is the Fourth Assessment Report released in 2007. Most AOGCMs have output for three divergent emissions scenarios (A1B, A2, and B1) that describe different future worlds with respect to demographic development, socio-economic development, and technical change, (IPCC, 2007). **Table 2** contains the complete list of AOGCMs used in this study, with their respective resolutions and available emission scenarios. Refer to Appendix A and B for AOGCM and SRES emission scenario descriptions, respectively.

CCCSN is sponsored by the Adaptation and Impacts Research Section (AIRS) of Environment Canada as well as various universities and other partners. It supports climate change and adaptation research in Canada by providing publicly accessible AOGCM and RCM output, downscaling tool downloads, and related research. An ensemble of six different AOGCMs are used in this study, each with their own biases. By simulating an ensemble of AOGCMs and considering all output to be equally possible, uncertainty is greatly reduced.

Table 1: Weather data used for model input

Model Input	Descriptions	Source	Input to
PPT	Daily precipitation amount (mm)	Environment Canada	LARS-WG, SDSM, KnnCAD
TMIN	Minimum daily temperature (°C)	Environment Canada	LARS-WG, SDSM, KnnCAD
TMAX	Minimum daily temperature (°C)	Environment Canada	LARS-WG, SDSM, KnnCAD
SR	Sun hours per day (h)	Lee, 2010	LARS-WG, SDSM
SPFH	Specific humidity	NARR	KnnCAD
UGRD	Eastward wind component (m/s)	NARR	KnnCAD
VGRD	Northward wind component (m/s)	NARR	KnnCAD
PRMSL	Mean sea level pressure (pa)	NARR	KnnCAD

Table 2: SRES Scenarios available for each AOGCM model

AOGCM Model	Sponsor	Country	Available SRES Scenarios	Atmospheric Resolution (Lat x Long)
CGCM3T47 (2005)	Canadian Centre for Climate Modelling and Analysis (CCCma)	Canada	A1B, A2, B1	3.75° x 3.75°
CGCM3T63 (2005)				2.81° x 2.81°
CSIRO MK3.5 (2001)	Commonwealth Scientific and Industrial Research Organization (CSIRO)	Australia	A2, B1	1.875° x 1.875°
GISSAOM (2004)	NASA's Goddard Institute for Space Studies	USA	A1B, B1	3° x 4°
MIROC3.2HIRES (2004)	Centre for Climate System Research at the University of Tokyo, National Institute for Environmental Studies, and the Frontier Research Centre	Japan	A1B, B1	1.125° x 1.125°
MIROC3.2MEDRES (2004)				2.8° x 2.8°

5. METHODOLOGY

The objective of this study is to perform a detailed analysis of LARS-WG for both baseline and future climate variables, as well as a comparison of future precipitation output from LARS-WG, SDSM, and KnnCAD for a single site in the Upper Thames River watershed. Each model uses historical datasets as input, and is capable of simulating a daily time-series of weather of infinite lengths. For the purpose of this study 27 years of historical climate data is used as input, and 324 years of daily climate variables are generated for the historical climate as well as for the 15 different AOGCM scenarios.

5.1 Model Calibration and Validation

Before simulating future climate for analysis, each downscaling tool must be calibrated and validated. LARS-WG, SDSM, and KnnCAD follow the same general validation procedure. Half the historical dataset is used as input to generate 324 years of daily weather for the baseline time period. That output is then compared to the remaining half of the historical data. If the simulated and observed results are statistically similar, the study may proceed. If not, adjustments to the model may be required. Since only 14 years (a half dataset) are available for validation, results may not be optimal as weather generators typically work best with 20-30 years of input.

5.2 Development & Application of Change Factors

The three stochastic models used in this study are capable of simulating future local climate variables in response to climate change by downscaling AOGCM output. This process

includes the interpolation of gridded AOGCM output to obtain data for a single site, followed by the modification of model input by applying change factors calculated from the AOGCM results.

$$w_1 = \frac{1/d_1^2}{1/d_1^2 + 1/d_2^2 + 1/d_3^2 + 1/d_4^2} \quad (5.1)$$

$$p_i(t) = \sum_{j=1}^4 w_j p_j(t) \quad (5.2)$$

Where i represents the station and j represents the grid point.

To obtain data for a single site, such as the London Airport, gridded AOGCM output is interpolated using the Inverse Distance Weighting method (IDW). First, the four grid points enclosing the site of interest are selected and the distance between grid points and the site are computed individually. Using Equation 5.1 each grid corner is assigned a weight, w , based on its distance to the site. A closer grid point will have a higher weight than one further away, and the sum of the resultant weights should equal '1'. Equation 5.2 is then used to interpolate the climate variable, p , for the site of interest. For example, to interpolate precipitation amount, the precipitation values for all four grid points are multiplied by their respective weights, then the four products are summed to obtain the final interpolated precipitation amount. In the end, the value of the closest grid point is most influential.

To calculate change factors, monthly weather data must be extracted from an AOGCM for both baseline and future time periods. The baseline period represents current weather and future time periods include 2020, 2050, and 2080 outputs for the purpose of this study. For precipitation and humidity, change factors are the percent change between future and baseline values and are multiplied by the daily values for each month. For all other variables, the change

factors are calculated as the magnitude of change and are added to the daily values for each month.

5.3 LARS-WG

Long Ashton Research Station Weather Generator, or LARS-WG, was developed by Semenov and Barrow (1997). The first step to using LARS-WG is to prepare historical weather input files that are used to calibrate the model. During calibration, LARS-WG analyses observed weather to determine its statistical characteristics and create site specific cumulative probability distributions (CPDs) for the various climate variables including wet and dry spell lengths, daily precipitation amount, minimum and maximum temperature, and solar radiation, (Semenov and Barrow, 2002).

Each CPD is divided into twenty-three intervals of climate variables ranging from minimum to maximum values. For each climate variable, v , there is a corresponding probability of occurrence, p .

$$p_0 = 0, \text{ and corresponds to } v_0 = \min\{v_{\text{obs}}\}$$

$$p_n = 1, \text{ and corresponds to } v_n = \max\{v_{\text{obs}}\}$$

To approximate extreme climate variables, p is set to 0 for minimum and 1 for maximum values. The remaining values are evenly distributed on the probability scale. To put this into perspective, the wet spell lengths for the winter season (December, January, and February), range from 0-18 consecutive days in the 27 years of historical data. There is a 31.0% probability that a 1 day wet spell will occur, a 56.0% probability that at most a 2 day wet spell will occur, and a probability of 68.5% that at most a 3 day wet spell will occur. This progression continues

until finally there is 100% probability that at most an 18 day wet spell will occur in the months of December, January, or February, (LARS-WG, 2010).

The wet and dry spell length distributions determine the precipitation status of each day, from which the other climate variables such as precipitation amount and temperatures are conditioned upon. Two CPDs exist for each conditional climate variable, one for a wet and the other for a dry day. Such variables are selected from separate distributions to maintain the multivariate correlation that exists between precipitation and other climate variables. For example solar radiation and temperature are both related to amount of cloud cover, and more coverage is expected on a wet day. Minimum and maximum temperature CPDs are a new feature of Semenov's latest model LARS-WG 5.0 which was used in this study (LARS-WG, 2010). Previous versions of LARS-WG normalized temperatures resulting in a poor estimation of future extremes in regions where temperatures do not follow such normal distributions. As mentioned earlier, CPDs are flexible and capable of fitting a variety of distributional shapes (Qian, 2004; Semenov 2002).

Once LARS-WG has been calibrated a series of synthetic daily weather may be generated. A random number generator selects climate variables from the CPDs, and as a result the synthetic weather will have the same statistical characteristics as the historical dataset. The generation process requires selection of the number of years to be simulated, as well as a random seed which controls the stochastic component of the weather generation. Different random seeds produce the same weather statistics, however variables differ on a day to day basis, (Semenov and Barrow, 2002).

5.4 SDSM

Statistical Downscaling Model (SDSM), developed by Wilby *et al.* (2002), incorporates both stochastic weather generation and regression based methods. It simulates local daily weather variables based on the assumed statistical relationship between observed local-scale "predictand" variables and large-scale atmospheric "predictor" variables, (Wilby and Dawson, 2007; Koukidis and Berg 2009). The first step to using SDSM is determining which predictors, such as humidity and wind speeds, are most strongly correlated to the local predictands required for the study including precipitation amounts and temperatures. This is achieved through the "screening variables" step in the program, where scatter plots and correlation analysis are used to determine the most appropriate combination of predictors. It is also beneficial to understand the physical relationships between large and small scale weather variables to ensure reasonable combinations are used, (Dibike and Coulibaly, 2005; Wilson and Dawson 2007).

The selected correlations are presented in the form of regression equations, and used to predict watershed scale variables from AOGCM output. Transfer functions can be used to improve such predictions as well. For example, a fourth root transformation is used to normalize the skewed daily precipitation distribution, while temperatures are normally distributed so the application of transfer functions is not required (Wilby and Dawson, 2007). As with LARS-WG, precipitation amount is first conditioned upon the wet or dry status of the day, then simulated using its correlation with atmospheric variables and fourth order transfer functions. Temperature assumes a direct correlation between local and atmospheric variables and is not conditioned upon precipitation status.

In order to calibrate the model, 14 years of the historical dataset is used as input and the remaining 13 years of data is used to validate the resultant output. This process is repeated multiple times using various combinations of predictor-predictand variables to determine which

combination is best able to reproduce the observed climate statistics. Following this several more tests are run using a constant set of predictor-predictand combinations and varying the choice of appropriate transfer functions, as well as the bias correction and variance inflation values.

Outputs are again analysed to establish which values of bias correction and variance inflation produce the most desirable results. Note that bias correction adjusts errors in the sample mean estimate, and variance inflation alters the amount of white noise in the regression model, (Khan *et al.*, 2006).

5.5 KnnCAD

KnnCAD (Version 3) is a non-parametric weather generator developed by Eum *et. al* (2009). It uses the traditional K-nearest neighbours generation approach with an additional perturbation component to improve the simulation of extreme climate.

The K-NN approach simulates climate variables one day at a time by selecting a day of weather most similar to the current day's from a subset of the historical data. The user is first prompted to input the number of years of historical weather N and a temporal window w from which the weather will be selected. The temporal window should be chosen carefully during the calibration process to ensure seasonality is preserved. If a 14 day window is used, a subset of data is created from the 14 days surrounding that date in any year of the historical data set. The weather variables for the days within this subset are analysed through principal component analysis and their similarity to the current day is measured using the Mahalanobis distance metric. The closest K days are retained from this subset and one day is randomly selected as the next days' weather using a geometric probability distribution where higher weights are assigned to closer neighbours.

A major drawback of the traditional K-NN weather generators is their inability to produce unique output, as the historical data is essentially reshuffled. Perturbation of precipitation amounts is an additional component developed by Sharif and Burn (2006) to add variability to the output and enhance the generators ability to predict extreme values.

6. RESULTS

Three different weather generators are used to simulate 324 years of synthetic climate data that represent the historical climate as well as 15 different AOGCM-modified future climates. This section includes validation, a detailed performance evaluation, and future simulation results from LARS-WG. For comparable detailed results from SDSM and KnnCAD refer to (Sarwar *et al.*, 2012) and (King *et al.*, 2010) respectively.

Before running simulations of future climate variables, LARS-WG must undergo validation and a performance evaluation for the specific site. The goal of any weather generator is to simulate climate with the same statistical characteristics as the observed data. In order to investigate the effectiveness of the LARS-WG model, box plots and line graphs are used to visually interpret the results. Total monthly precipitation, total monthly number of wet days, and minimum and maximum temperatures are illustrated as box plots, while wet spell lengths are presented using frequency line graphs.

For this study box plots are a favourable method of presenting data for analysis as they clearly display statistical information. The height of the box represents the inter-quartile range, the horizontal line inside the box indicates the median, and the whiskers extend to the 5th and 95th percentiles of the simulated datasets. For the purpose of comparison, the median of historical climate data is plotted on top of the box plots as a line.

6.1 Validation and Performance Evaluation

Validation of LARS-WG is performed by using half the historical dataset as input to simulate 324 years of current climate data, and comparing that output to the remaining half of the historical data. Since the historical data consists of 27 years, the first 14 years (1979-1992) are used as input and the remaining 13 years (1993-2005) are left for comparison. During the validation process several graphs are constructed using outputs from four simulations with varied random seed values. The graphs are compared to determine which random seed gives the most accurate results. A value of 4409 is found to produce the strongest correlation with the observed data, therefore it is used throughout the entire study and the others were omitted. **Figure 2** shows the comparison between random seeds 541, 1223, 2741, and 4409 for the simulation of total monthly precipitation which is the most influential climate variable in a hydrologic impact assessment. For this particular climate variable statistics are quite uniform between all random seed results.

Following validation, a performance evaluation is done using the full 27-year observed record to determine how well LARS-WG reproduces observed climate characteristics. **Figure 3** contains box plots of simulated total monthly precipitation with historical medians shown as a line plot. It is evident that the observed and simulated data are in close agreement as all observed medians lie within the inter-quartile ranges of the observed data. In most months the historical median agrees with that of the simulated data. The plot for total number of wet days shows similar results in **Figure 4**. Again, all observed values lie within the simulated inter-quartile

range, however LARS-WG slightly underestimates results for January, March, June, August, September, and December, and overestimates results for February, May, July, and October.

The temperature box plots differ in that there is far less monthly variation in average temperature. **Figure 5** and **Figure 6** contain minimum and maximum temperature results, respectively. The inter-quartile boxes and whiskers are quite short, and any outliers are just outside the 5th and 95th percentiles. Most results lie within the simulated inter-quartile range, and the observed medians agree closely with the simulated values. There is a slight overestimation in the maximum average temperature predicted for February and August and an underestimation in January. Overall, LARS-WG reproduces both minimum and maximum average daily temperatures fairly well.

Wet spell lengths are relatively well simulated, however in some months one-day spell lengths tend to be underestimated, and two-day spell lengths are overestimated. **Figure 7** contains such poorly simulated results for July, while **Figure 8** depicts results for September which is a well-simulated month. May, June, October, November, and December have similar results to July, while January to April are simulated more accurately, as in September.

Based on these results, LARS-WG's performance in simulating historical climate is deemed acceptable and it may be used to simulate future climate variables for analysis.

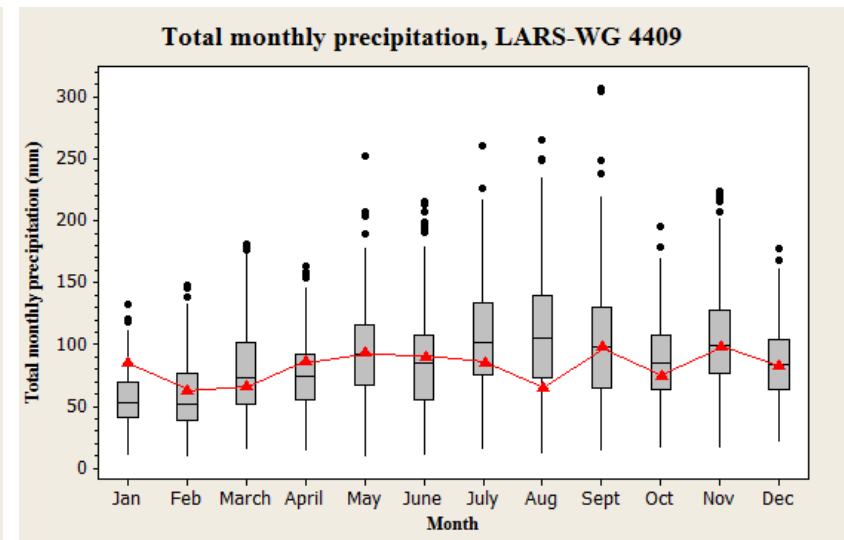
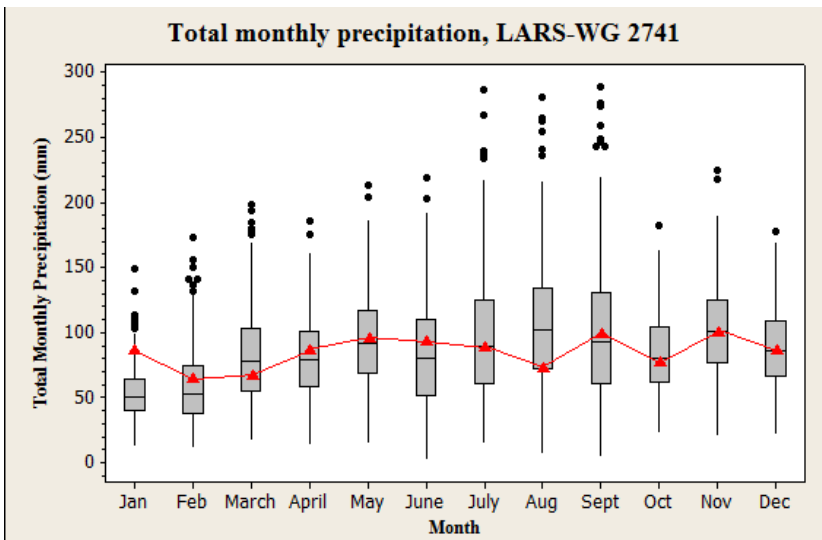
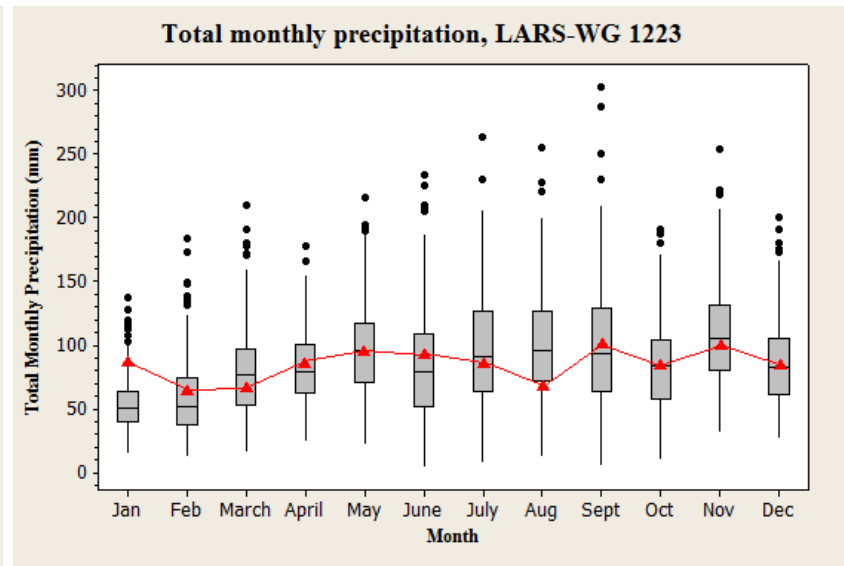
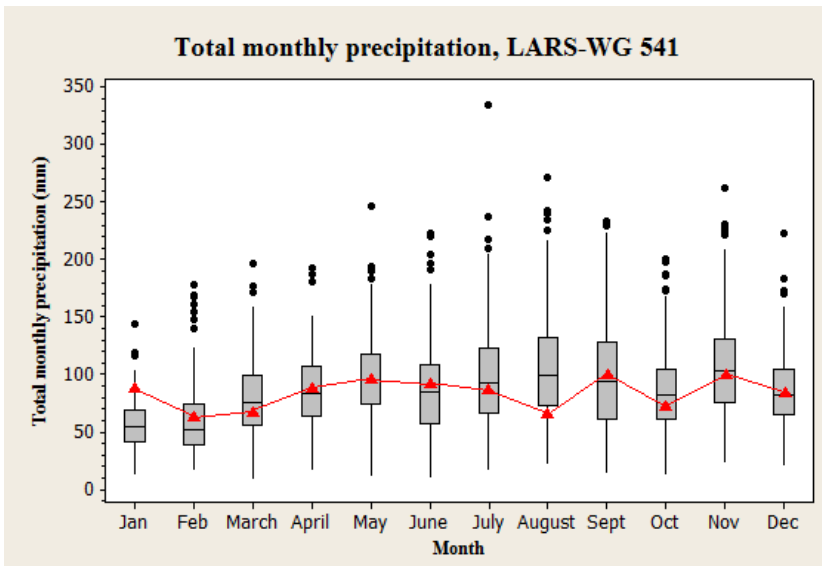


Figure 2: Validation results for total monthly precipitation using 541, 1223, 2741, and 4409 random seeds.

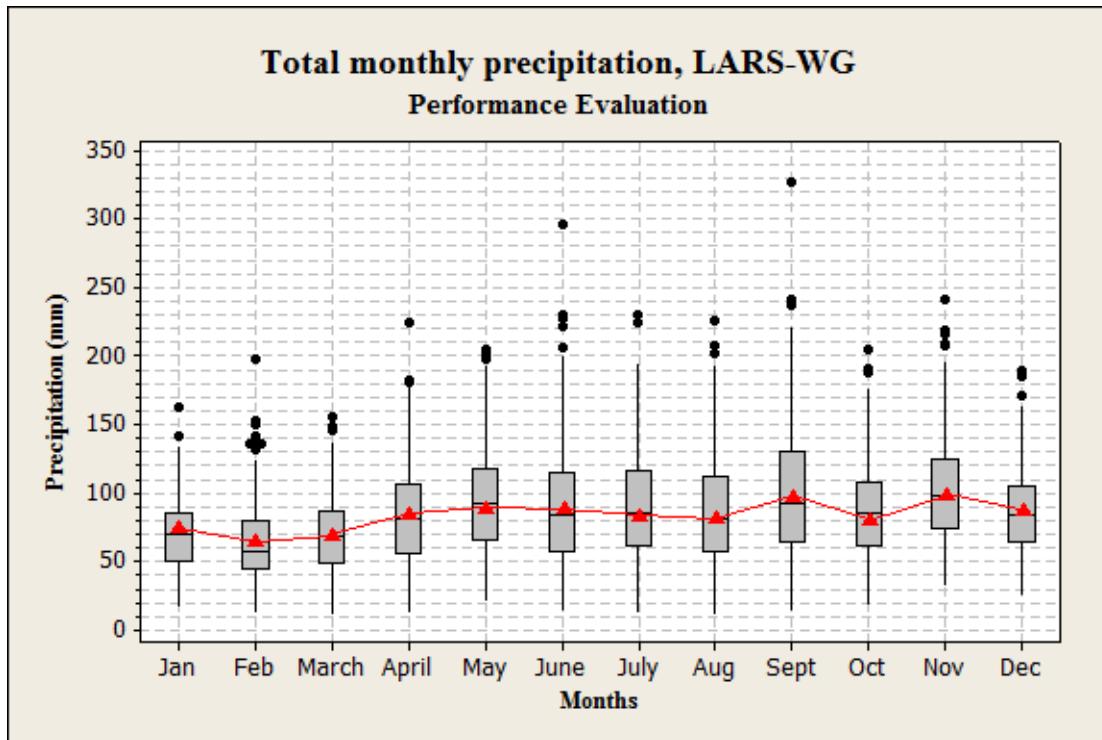


Figure 3: LARS-WG performance evaluation results for total monthly precipitation.

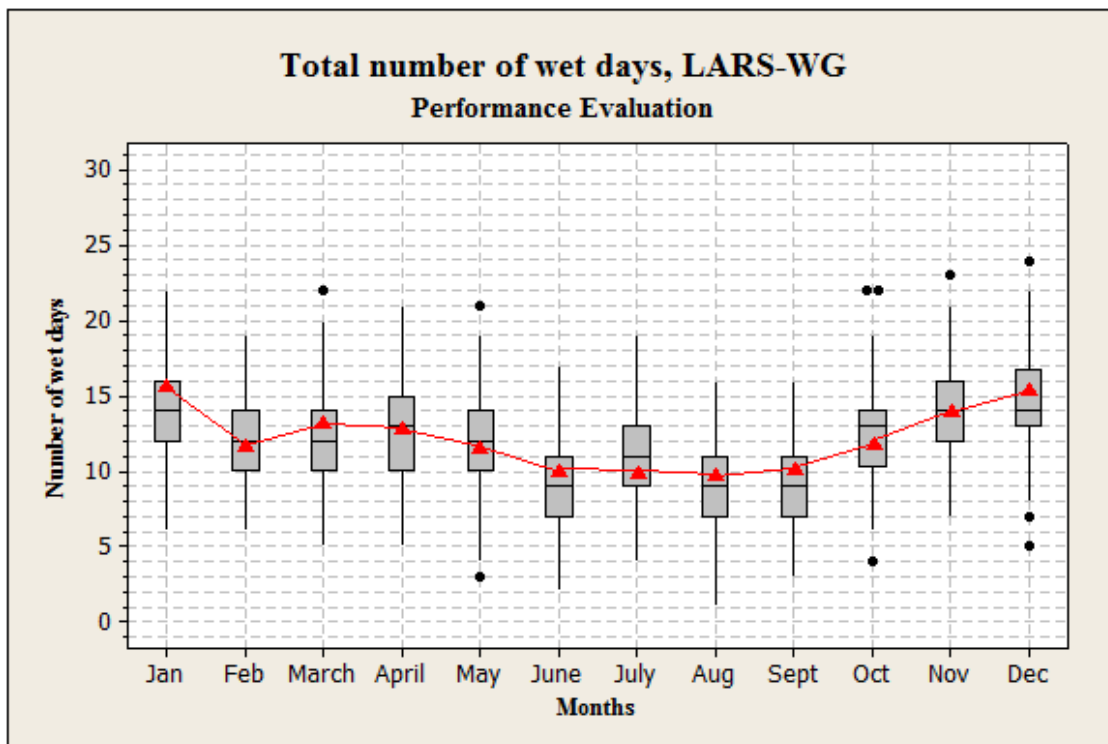


Figure 4: LARS-WG performance evaluation results for total number of wet days.

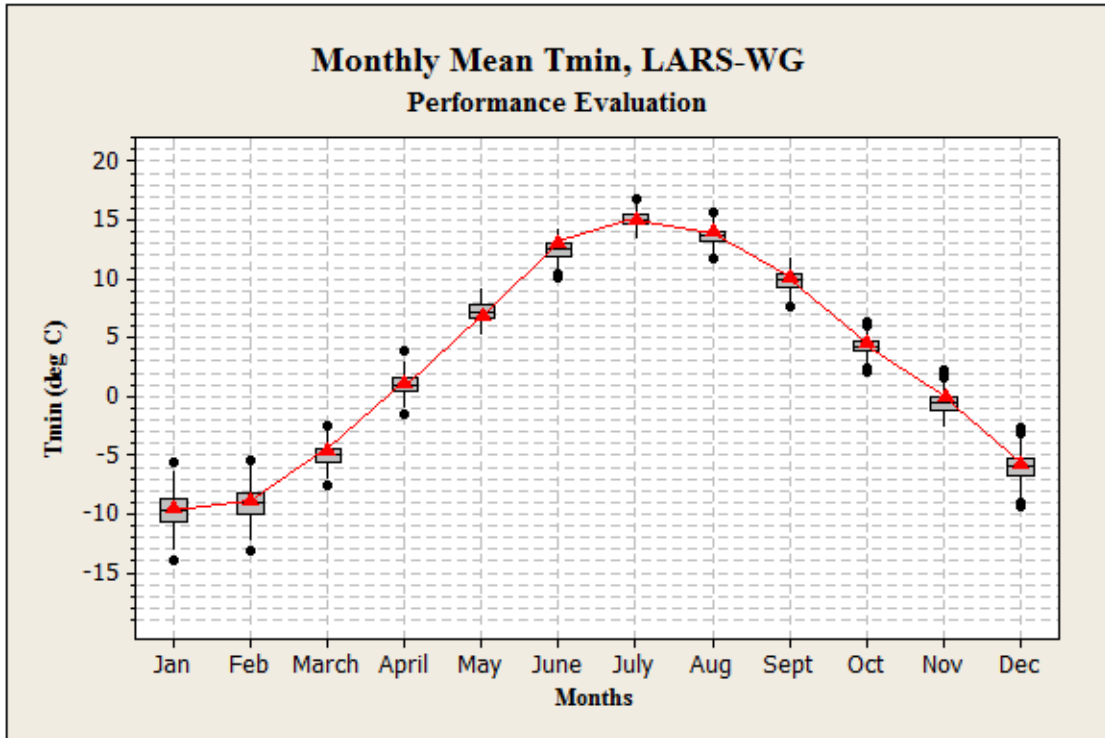


Figure 5: LARS-WG Performance evaluation results for minimum temperature.

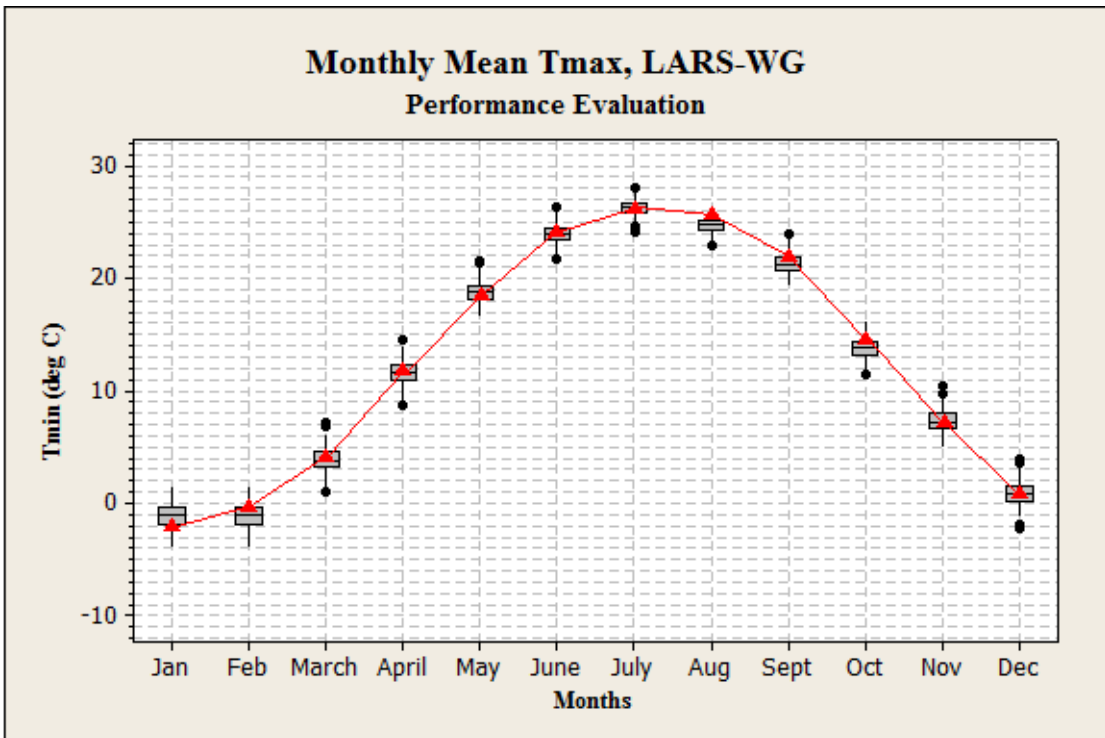


Figure 6: LARS-WG performance evaluation results for maximum temperature.

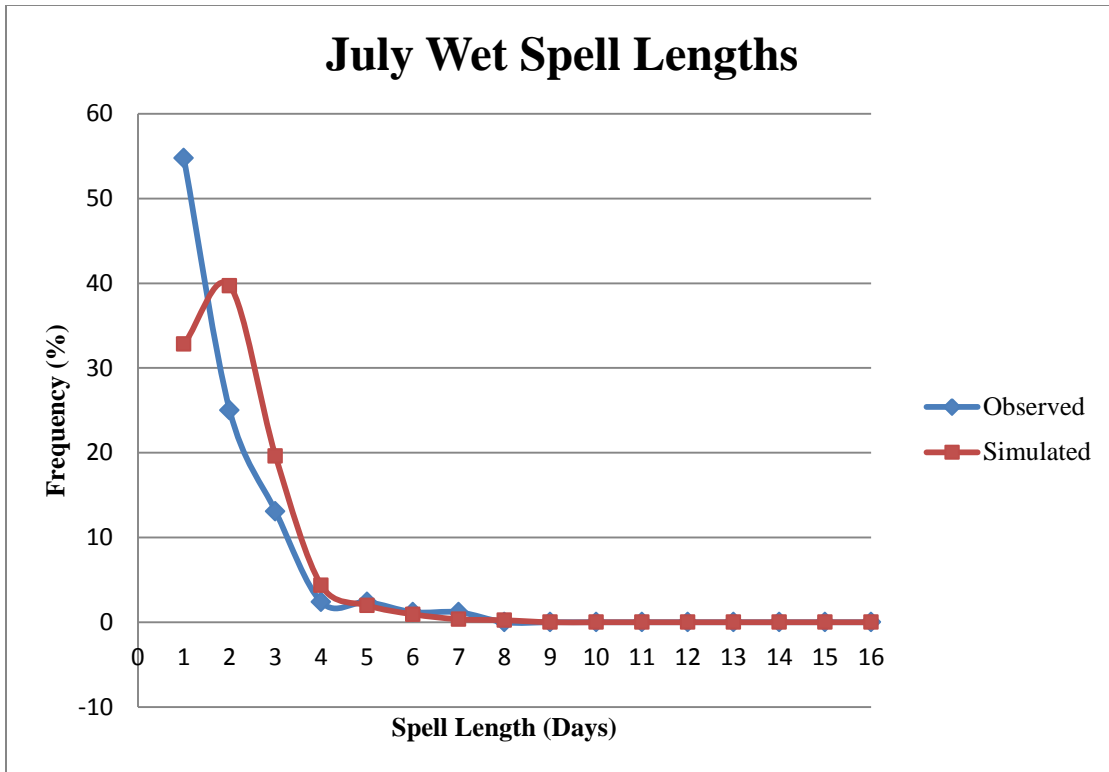


Figure 7: LARS-WG fair performance evaluation results for wet spell lengths in July.

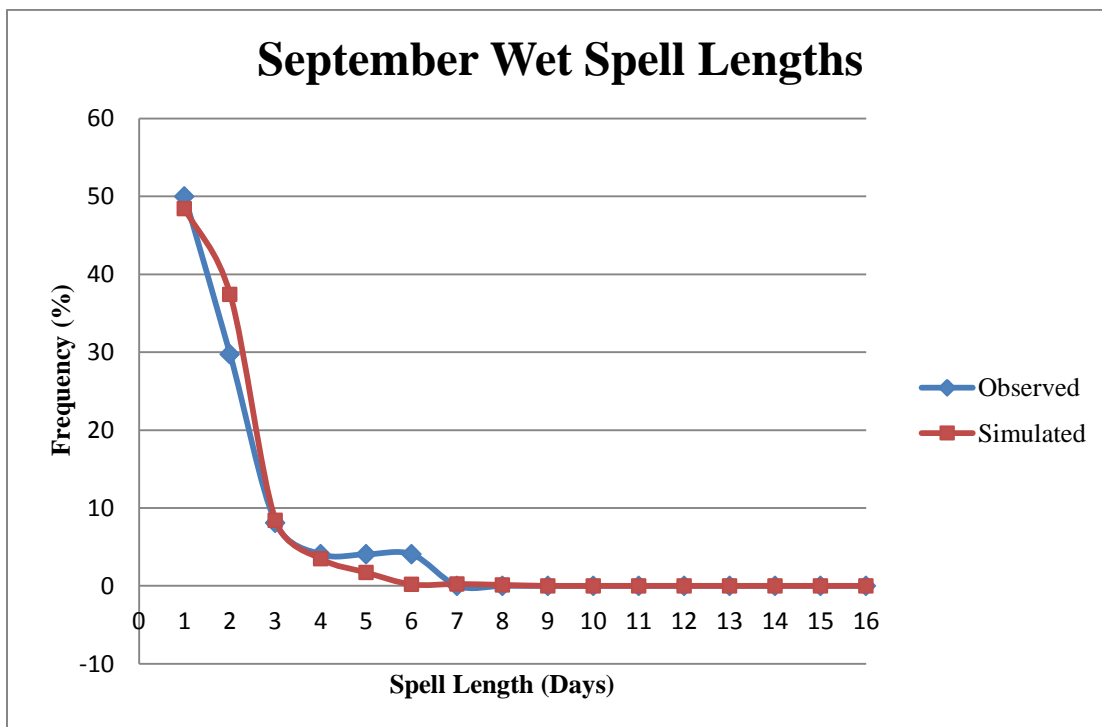


Figure 8: LARS-WG successful performance evaluation results for wet spell lengths in September.

6.2 Generation of Future Climate Variables

In order to simulate the future climate, change factors are used to modify the historical input parameters. Output from six AOGCMs are used to create change factors for the 2020, 2050, and 2080 time periods; refer to **Table 2**.

The resultant monthly change factors are applied to the 27 years of historical weather input, and a 324 year time-series is simulated for each AOGCM in all three future time periods. This report provides a detailed analysis of the future climate produced by LARS-WG for the 2020 and 2080 time periods. The 2050 results are excluded from this section to avoid redundancy and may be found in **Appendix C**.

6.2.1 Total Monthly Precipitation

Percent change charts are developed to visualize how each AOGCM projects an increase or decrease in total monthly precipitation relative to observed weather data. A positive value indicates an increase and a negative value indicates a decrease in total precipitation. A zero percent change indicates no change between future and observed parameters. Three charts are created to represent the 2020, 2050, and 2080 time periods. The 2020 and 2080 results are available in **Figure 9** and **Figure 10**, while 2050 results are available in **Figure 18** in **Appendix C**.

It is evident that some discrepancy exists between the models as both positive and negative changes of varying magnitudes are predicted for each monthly value. However, there are groups of months that exhibit similar trends. In the late winter and spring (February, March, April, May) the majority of AOGCMs agree that total monthly precipitation will increase between less than 1% to 33.5% in the 2020 time period. The highest value is predicted by

CGCM3T63 A2 scenario in May. In fact all models predict positive results in May for the 2020 time period. However, seasonally there are several models that project negative results. In February all scenarios driving CGCM3T63 project a decrease in precipitation between 1% to 16%, which are the most significant negative results for the season.

The opposite is true for summer and early fall (June, July, August, September), as thirty-two of the sixty AOGCM simulations predict a decrease in precipitation in the 2020 time period. In June the CGCM3T47 and CGCM3T63 models predict decreases between 2% to 22% for A1B, A2, and B1 scenarios. MIROC3.2HIRES A1B also projects a significant decrease of 26%, which is the largest decrease predicted for the season. Models project relatively moderate positive and negative values for July and August, while September results are more extreme. All scenarios for CGCM3T47, CSIROmk 3.5, and MIROC3.2MEDRES, as well as GISSAOM A1B and MIROC3.2HIRES B1 project negative results between 3% to 20%. On the other hand, CGCM3T63 A1B predicts the greatest increase in precipitation for the entire season at 37%.

Finally, in late fall and early winter (October, November, December, January) more models project an increase than a decrease in precipitation, and the magnitudes of increase are greater. In the 2020 time period October, November, and December have similar results, while January is more unique. All scenarios driving CGCM3T47 and CGCM3T63 project increases in precipitation between 1% to 55% for October, November and December. CGCM3T47 A2 in October, and CGCM3T63 A1B and A2 in November all predict increases in precipitation greater than 50%. Conversely, CSIROmk 3.5 B1 projects the greatest decrease in precipitation at 28% for the October 2020 time period. Results for January are more sporadic, and both positive and negative values are relatively insignificant.

These patterns are more pronounced in the 2080s as changes become more extreme further into the future; refer to **Figure 10**. For the late winter and spring all models project an increase in precipitation with the exception of MIROC3.2MEDRES B1 in February, and MIROC3.2HIRES A1B and B1 in May. The negative changes in precipitation are small, while positive results range from 1% to 48%. The 48% increase is predicted by CGCM3T63 A1B in March.

The 2080 results for summer and early fall are evenly split between positive and negative values, however the magnitudes of precipitation increase are less, while the magnitudes of precipitation decrease are significantly greater. All scenarios driving MIROC3.2MEDRES project precipitation decreases between 2% to 48% for June, July, August and September. The 48% decrease is predicted by MIROC3.2MEDRES A1B in September, which continues to be the month providing the most extreme negative results. Notably, MIROC3.2MEDRES A1B also predicts a precipitation decrease of 36% for August.

The number and magnitude of predicted precipitation increases are higher in the late fall and early winter 2080 time period. Only eight of the sixty AOGCMs project precipitation decreases, which are all less than 20% for the season. All scenarios for CGCM3T63 project extreme precipitation increases for October, and November especially, ranging from 34% to 76%. The 76% increase is predicted by CGCM3T63 A1B in November. Predicted increases in December and January are relatively moderate, as they range from approximately 1% to 32%.

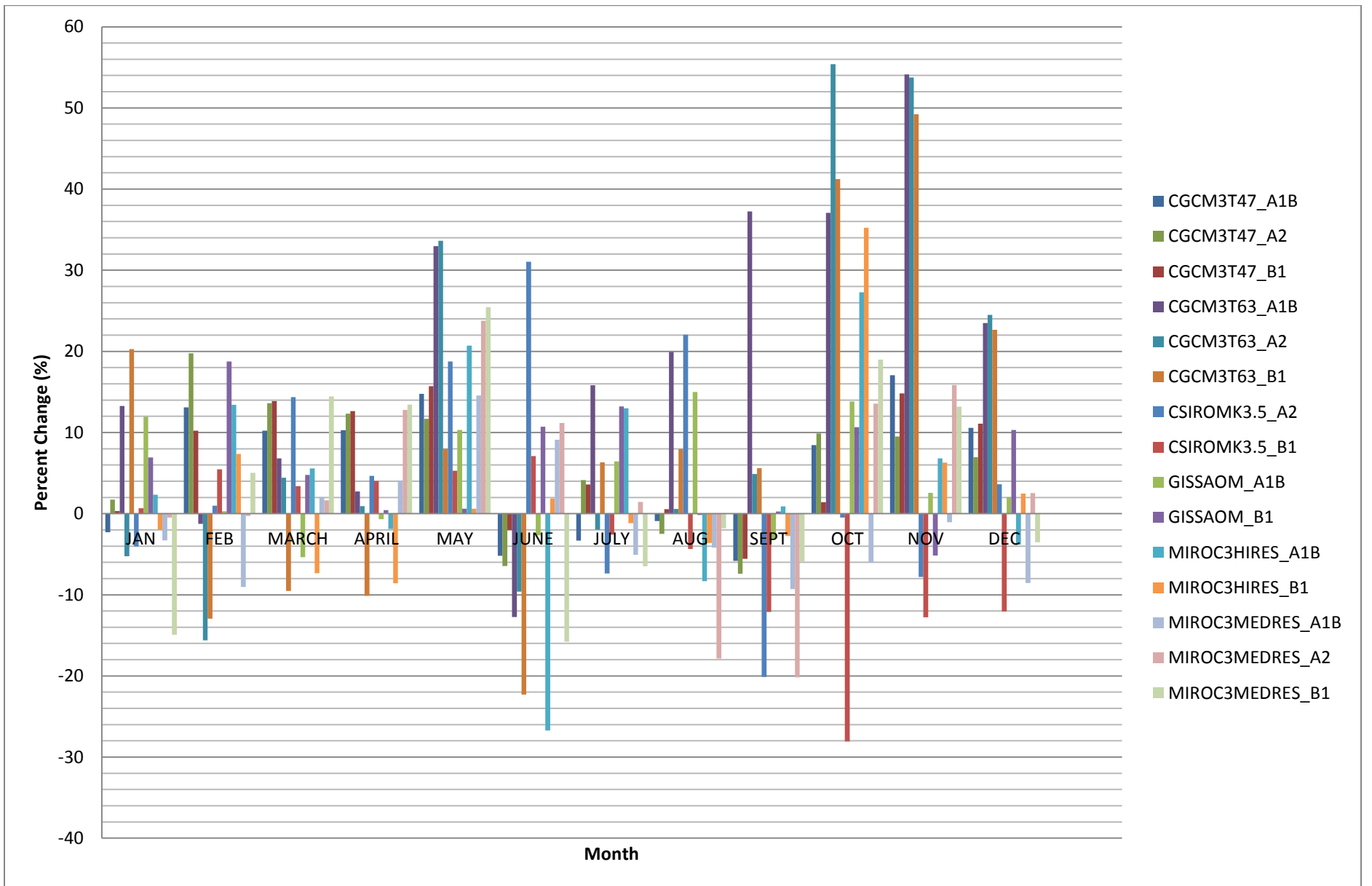


Figure 9: Percent change in total monthly precipitation, 2020s.

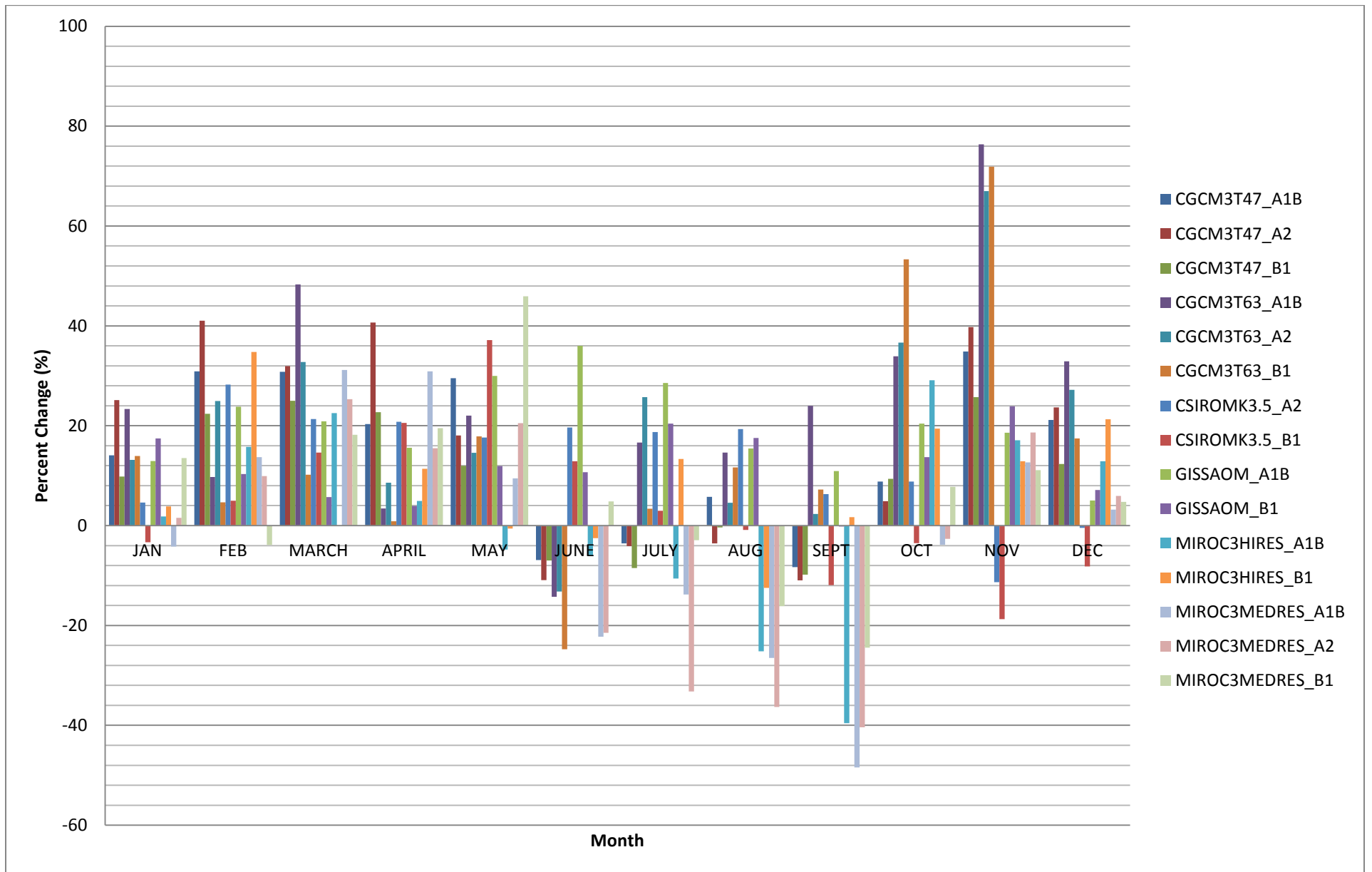


Figure 10: Percent change in total monthly precipitation, 2080s

6.2.2 Total Monthly Number of Wet Days

The percent change between baseline and future climate is also used to analyze change in total monthly number of wet days. Three percent change graphs represent the 2020, 2050, and 2080 future time periods. The 2020 and 2080 results are available in **Figure 11** and **Figure 12**, while 2050 results are in **Figure 19** in **Appendix C**. AOGCMs tend to predict similar results within each month, however results vary greatly between months. In the following analysis the first paragraph describes 2020 results, while the second explains the 2080s.

In January all AOGCMs predict a decrease in total number of wet days between baseline and 2020 time periods. Results range from -9% to -13%, with the exception of a more significant 17% decrease projected by MIROC3.2MEDRES A1B. There is little agreement among AOGCM outputs for February. The magnitudes of percent change are fairly moderate, excluding the 13% decrease in number of wet days projected by MIROC3.2MEDRES A1B. The months of March and August produce quite similar results. All AOGCMs and their respective emissions scenarios project a decrease between 3% to 12%. April provides mostly negative results up to around -11%. Results for May and July are also fairly similar in the 2020s. All models and their respective scenarios project an increase of around 2% to 14% for May, and 1% to 12% for July. In June thirteen of the fifteen models project a decrease in the number of wet days between 2% to 8.5%, while MIROC3.2MEDRES A1B predicts a 21% increase which is by far the highest increase for all months in the 2020 time period. September contains some of the most extreme results for both 2020 and 2080 time periods, as all AOGCM scenarios project a decrease between 8.5% to 21% in the 2020s. In October the majority of AOGCMs predict an increase in number of wet days between 2% to 11% while CSIROmk 3.5 B1 and MIROC3.2MEDRES A1B predict decreases of less than 1% and 8%, respectively. November also provides a mixture of results.

Positive results range from 1% to 10%, while negative projections are fairly insignificant. Finally all models project a decrease in total number of wet days between 2% to 10.5% for December.

Unlike the results for total monthly precipitation, the magnitude of change in total number of wet days does not seem to increase in the 2080s. In the January 2080 time period all models switch to predict positive results between 7% to 13.5%, indicating an increase in number of wet days as time progresses. February predictions continue to consist of fairly low increases between 1% to 11%, and one negative value of less than 1% projected by MIROC3.2HIRES A1B. The 2080 predictions for March and August are similar to those of the 2020s, as values range between a 3% to 13% decrease in number of wet days. In April, there is little change between baseline and 2080 time periods as most predictions are less than 1% and fluctuate between negative and positive values. Similar to March and August results, May and July provide little change between 2020 and 2080 results. Models predict increases of around 4% to 16% in May and 2% to 15% in July. In June the majority of models project negative results between 1% to 8%. September continues to exhibit more extreme magnitudes of change in the number of wet days, as predictions range from -14% to -17%. Such results correspond with the 48% decrease in total precipitation in the September 2080 time period; refer to Section 6.2.1. Results are fairly similar for October and November, with a strong agreement among AOGCMs that the number of wet days will increase up to 12%. Again, the 2020 and 2080 results are similar in sign and magnitude for December, as they range between a 2% to 8% increase. Overall, there are no obvious trends in the number of wet days as time progresses.

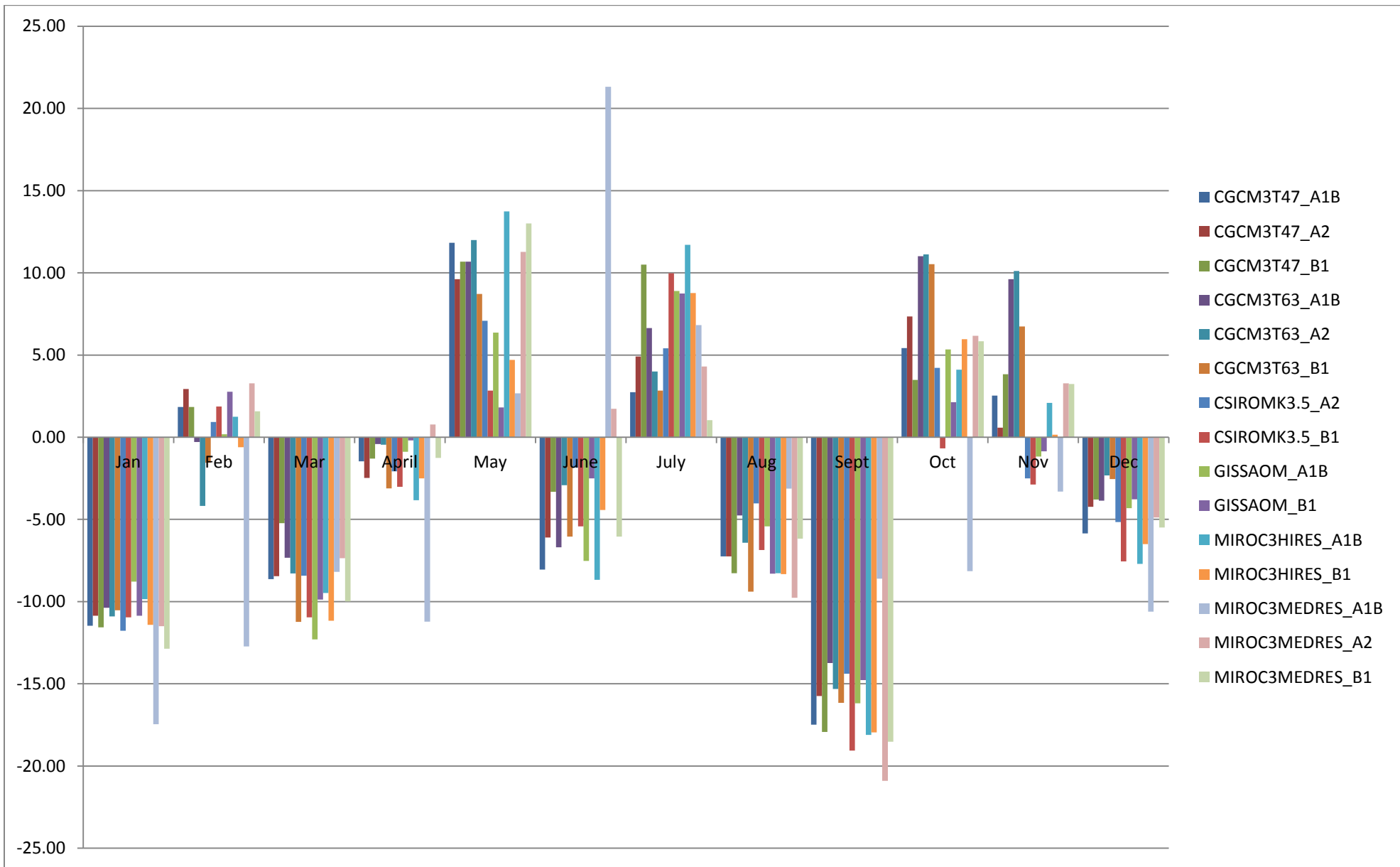


Figure 11: Percent change in total number of wet days, 2020s

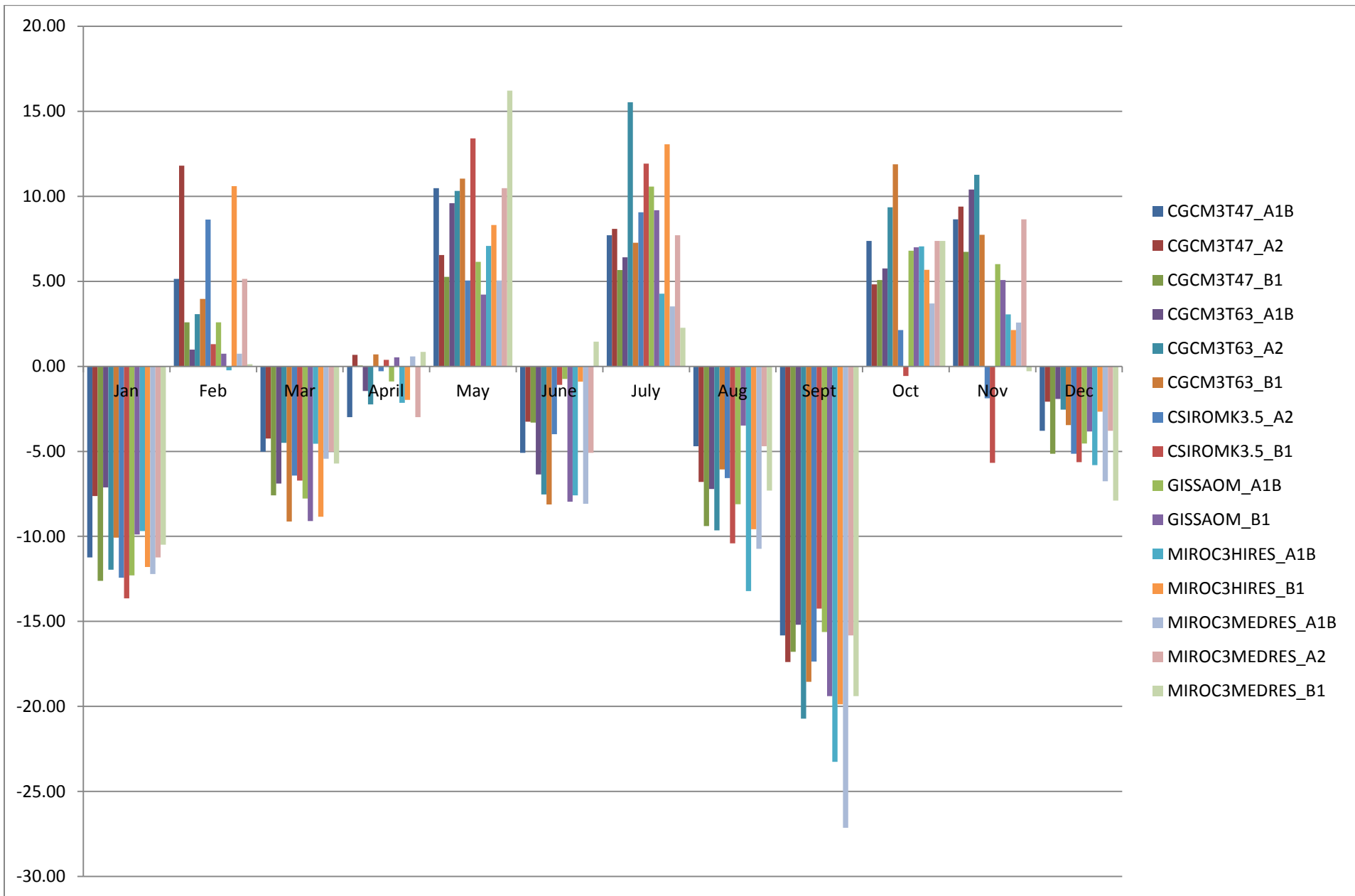


Figure 12: Percent change in total number of wet days, 2080s.

6.2.3 Temperature

The temperature results are presented as line graphs in **Figure 13** to **Figure 16** for the 2020s and 2080s. Minimum and maximum temperature plots are developed for 2020, 2050, and 2080 time periods for emission scenarios A1B, A2, and B1. Each plot has four to six lines that represent the various AOGCMs as well as a thicker black line representative of the historical climate. Plots for the 2050 time period are available in **Appendix C**.

For maximum temperature results in the 2020 time period, the three graphs representing A1B, A2, and B1 scenarios look quite similar. All lines follow a uniform bell curve shape and have a strong correlation, indicating a close agreement among AOGCM outputs. The low points of the curves occur in January, February, and December and the high points peaks in July. GISSAOM predicts higher temperatures in May than in June from both A1B and B1 scenarios, which may be due to AOGCM shortcomings or error in the calculation of the figure. In July MIROC3.2HIRES projects a significant maximum temperature of 28.4 °C for scenario A1B, while MIROC3.2MEDRES projects maximum temperatures of 28.1°C and 28.5°C for scenarios A2 and B1, respectively. To put these results into perspective, the average historical maximum temperature in July is 26.38°C.

The averaged minimum temperatures in the 2020 time period follow the same shape as the maximum temperatures. The greatest discrepancy between future and baseline values occurs in February for all three scenarios. The average historical minimum temperature in February is -9.1°C, while CGCM3T47 consistently projects the most extreme minimum temperatures as -5.74°C, -5.77°C, and -6.08°C for scenarios A1B, A2, and B1, respectively.

It is evident that the magnitudes of both maximum and minimum temperatures increase in the 2080s, as the gap between future and historical results grows wider. In addition, the future outcomes are more highly variable. The agreement between AOGCM simulations becomes weaker and the predicted values are more spread out. As in the 2020 time period, GISSAOM A1B and A2 projected lower temperatures for June than that for May for maximum temperature only. Although this trend is observed in both 2020 and 2080 time periods, 2050s values from the model appear to be more reasonable; **Appendix C, Figure 20**. This likely indicates an error in change factor application or perhaps within the AOGCM dataset.

The greatest discrepancy between baseline and 2080 average maximum temperatures occurs in March. The observed maximum temperature in March is 4.34°C, while MIROC3.2MEDRES consistently yields the most extreme results as 11.88°C, 13.12°C and 9.29°C for scenarios A1B, A2, and B1, respectively. For minimum temperature in the 2080 time period the gap between baseline and future results is widest in February. Again it is the MIROC3.2MEDRES model that projects the most extreme results of -1.25°C, -0.76°C, and -4.33°C for scenarios A1B, A2, and B1, respectively while the historical average minimum temperature is -9.13°C for that month.

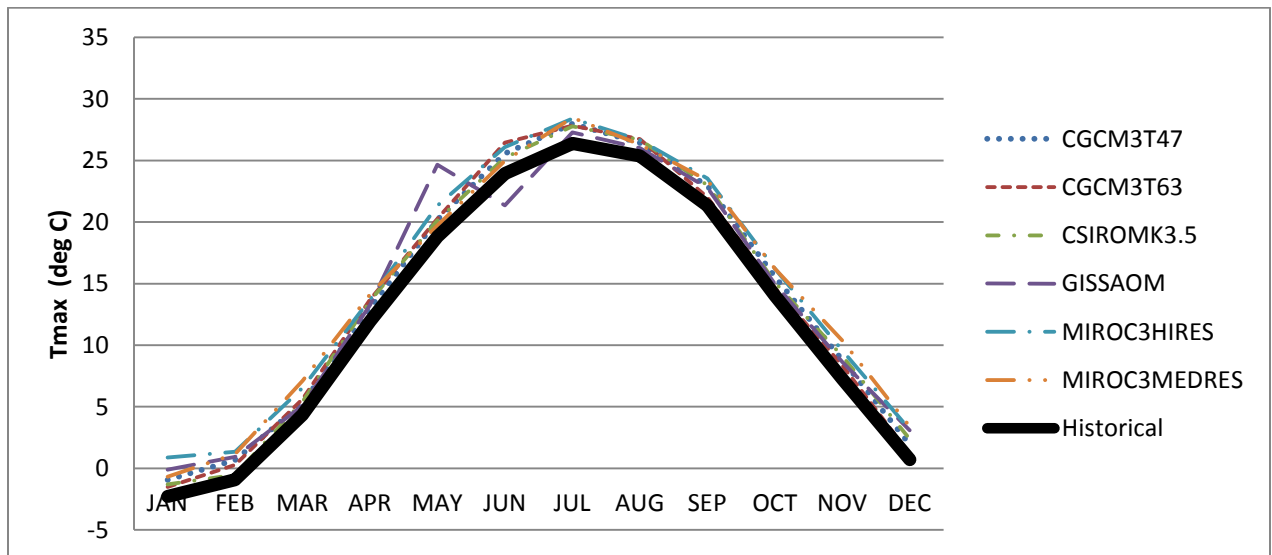
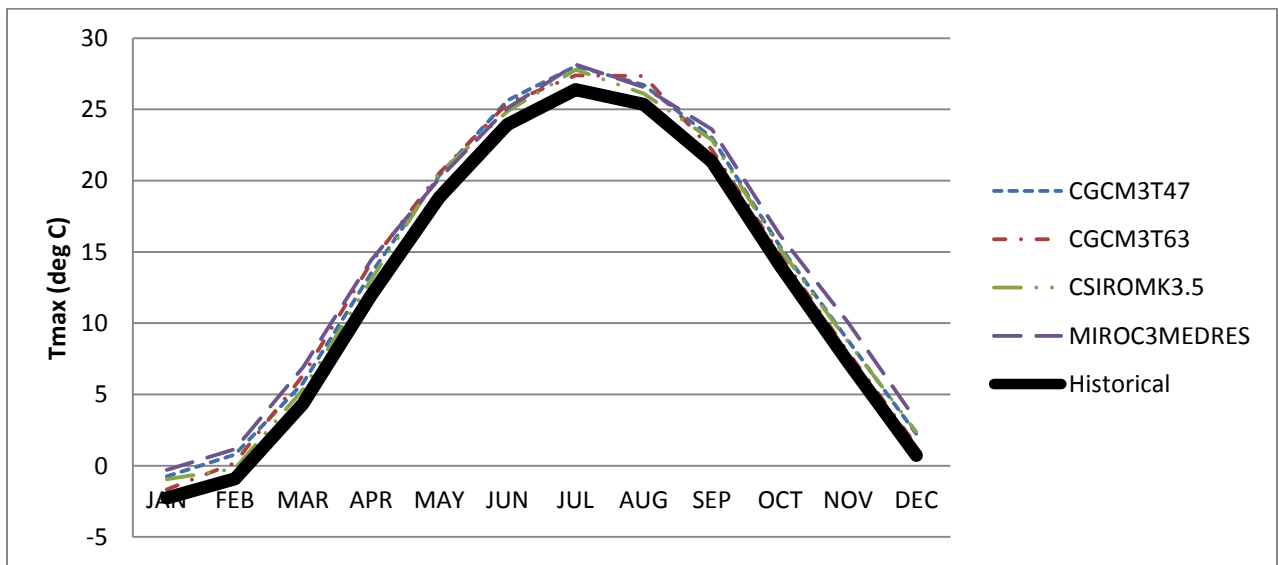
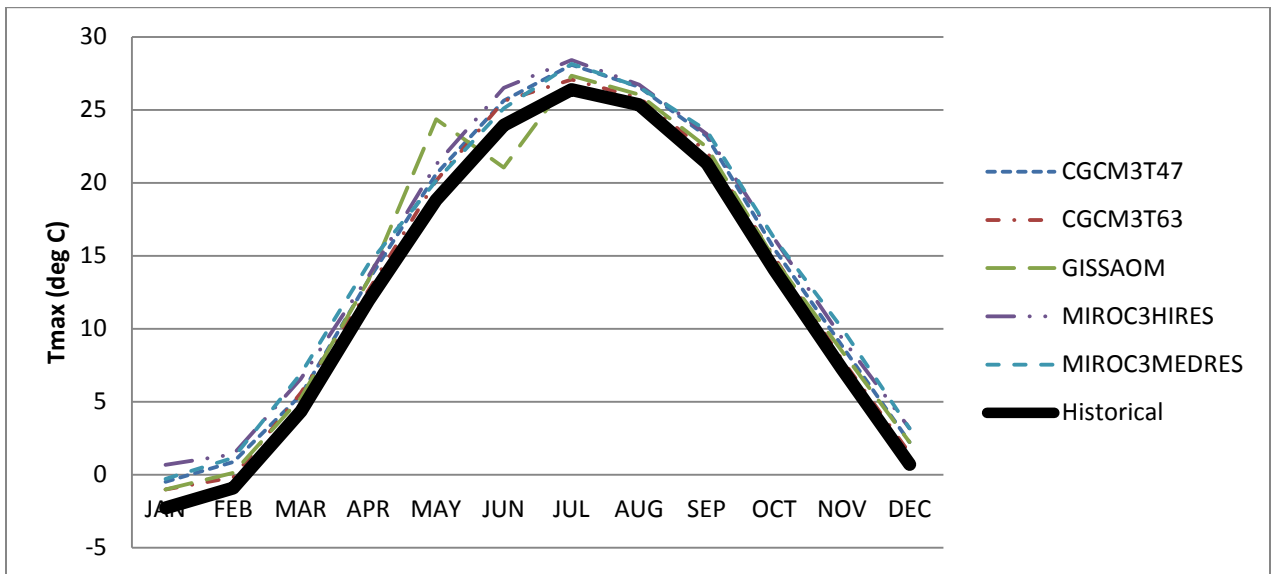
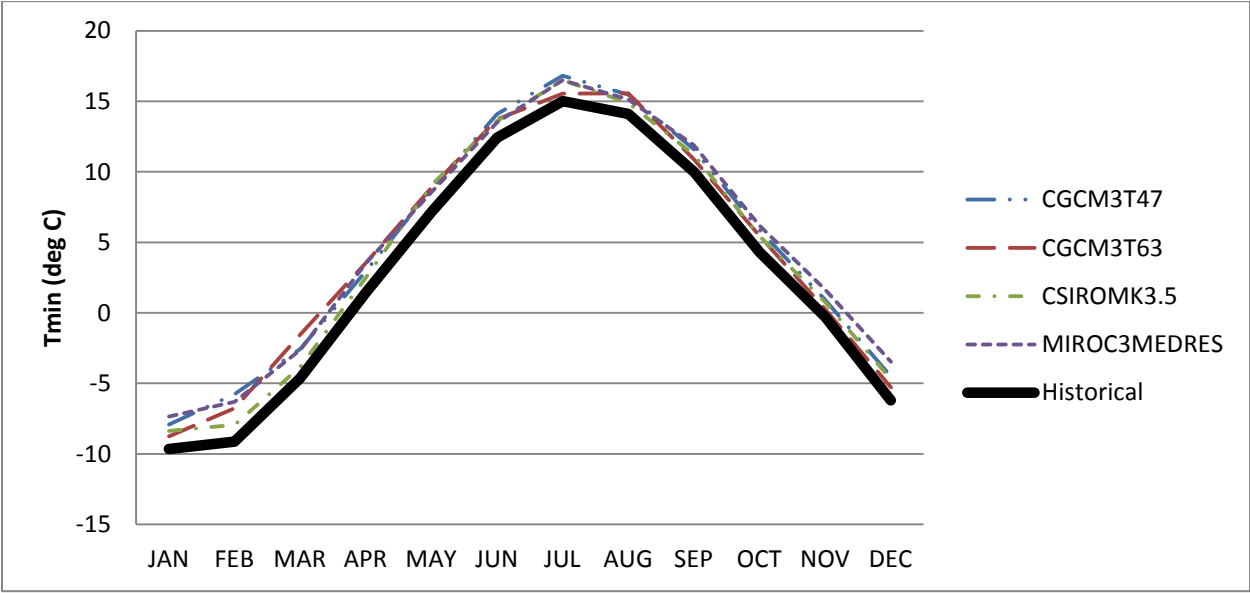
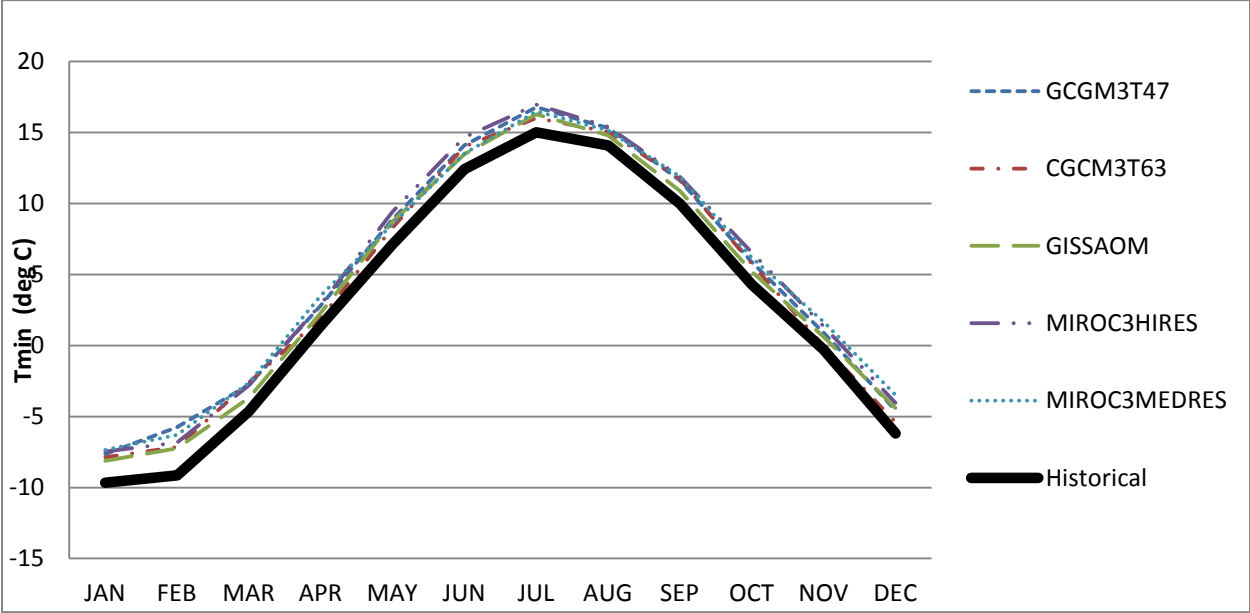


Figure 13: AOGCM predictions for maximum temperature, 2020s. Emission scenarios A1B, A2, B1 from top to bottom.



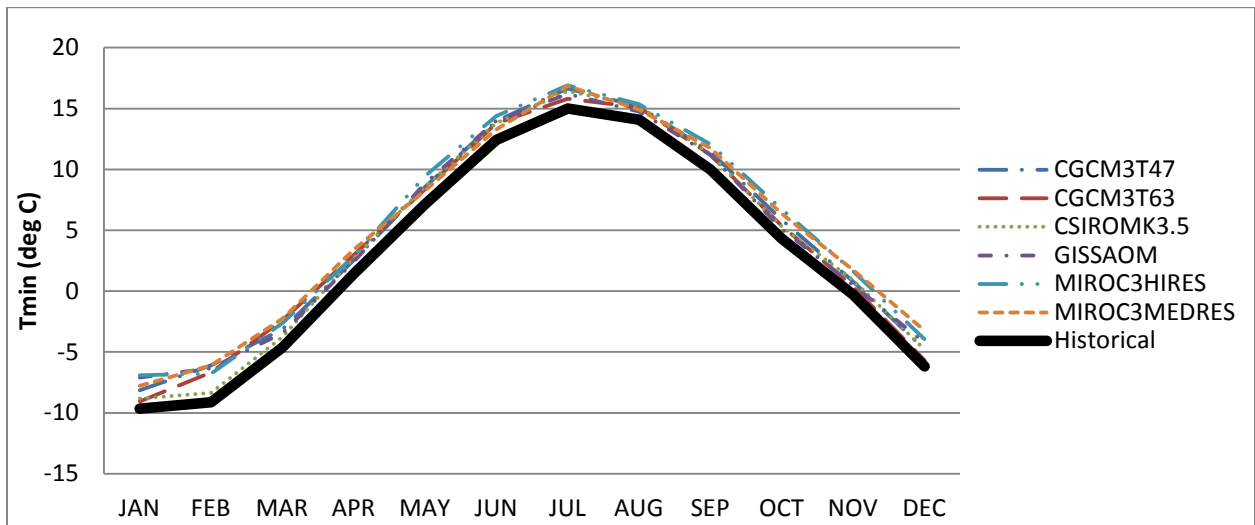
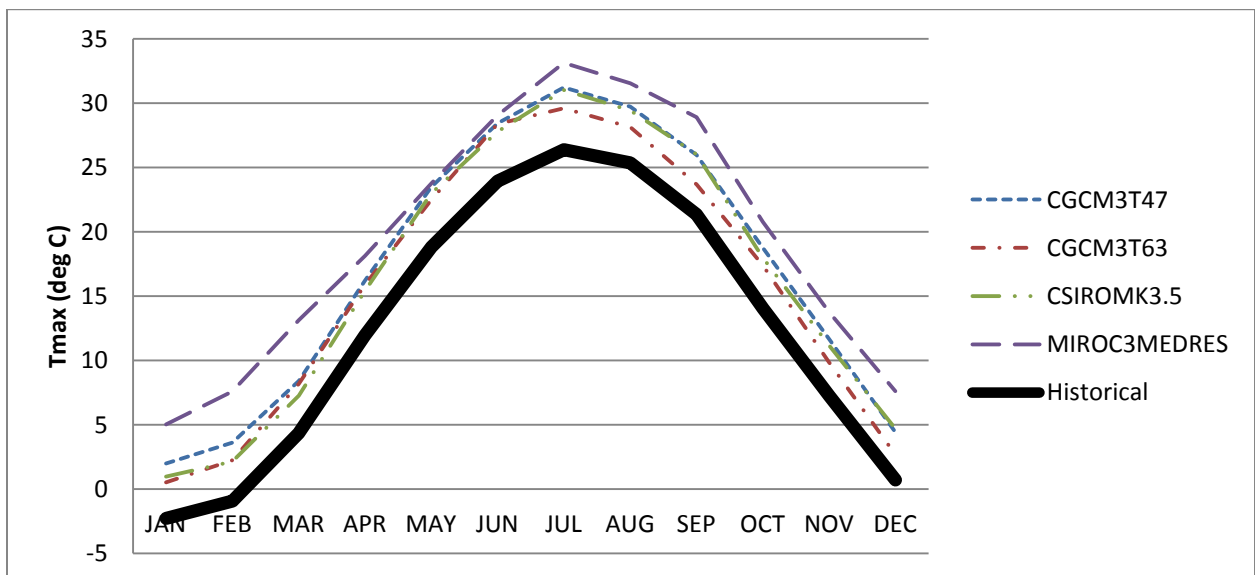
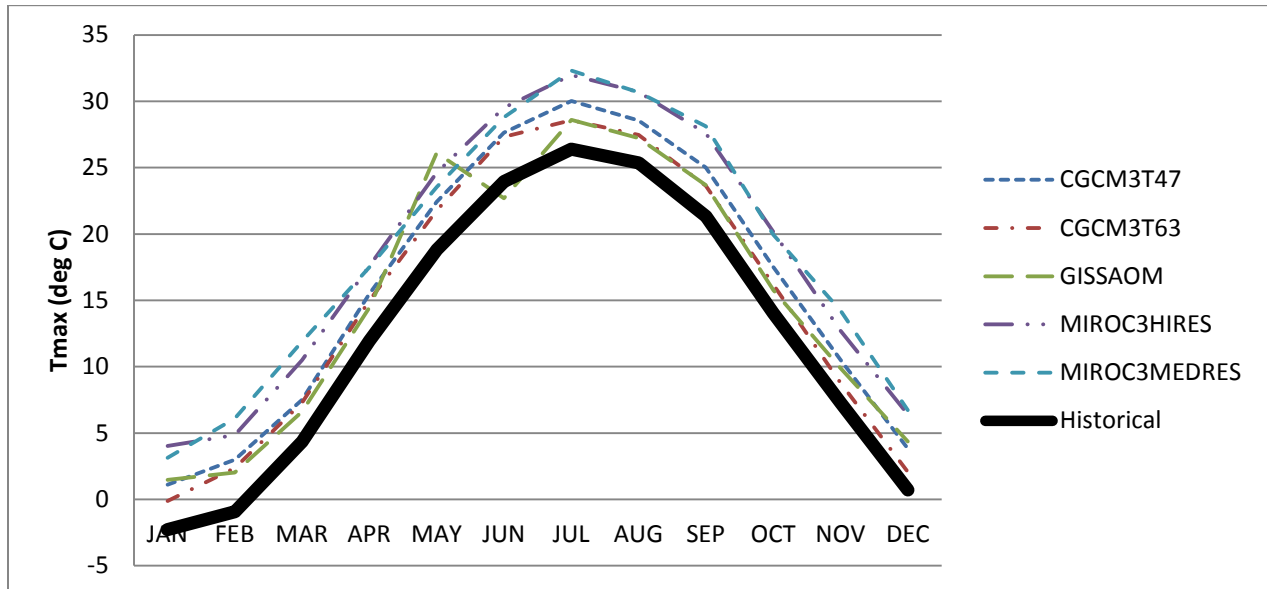


Figure 14: AOGCM predictions for minimum temperature, 2020s. Emission scenarios A1B, A2, B1 from top to bottom.



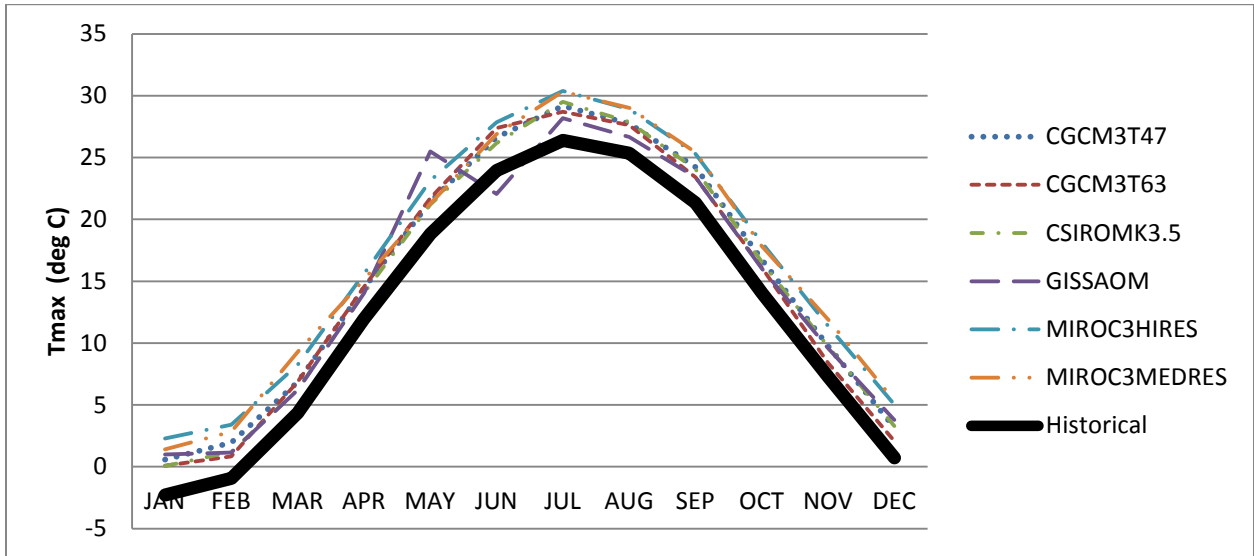
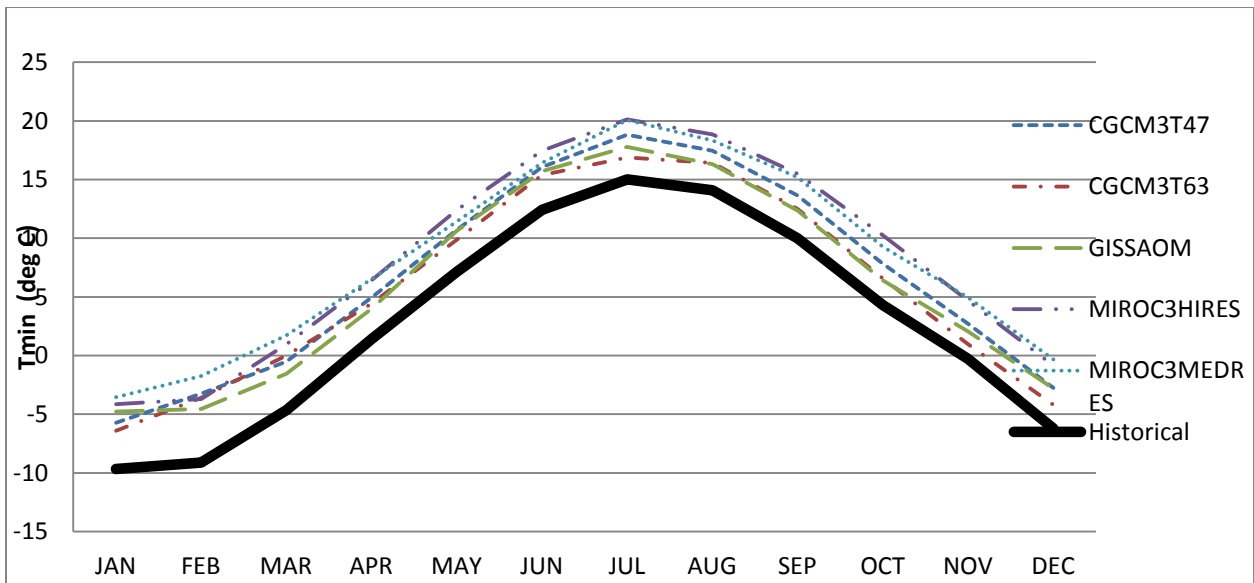


Figure 15: AOGCM predictions for maximum temperature, 2080s. Emission scenarios A1B, A2, B1 from top to bottom.



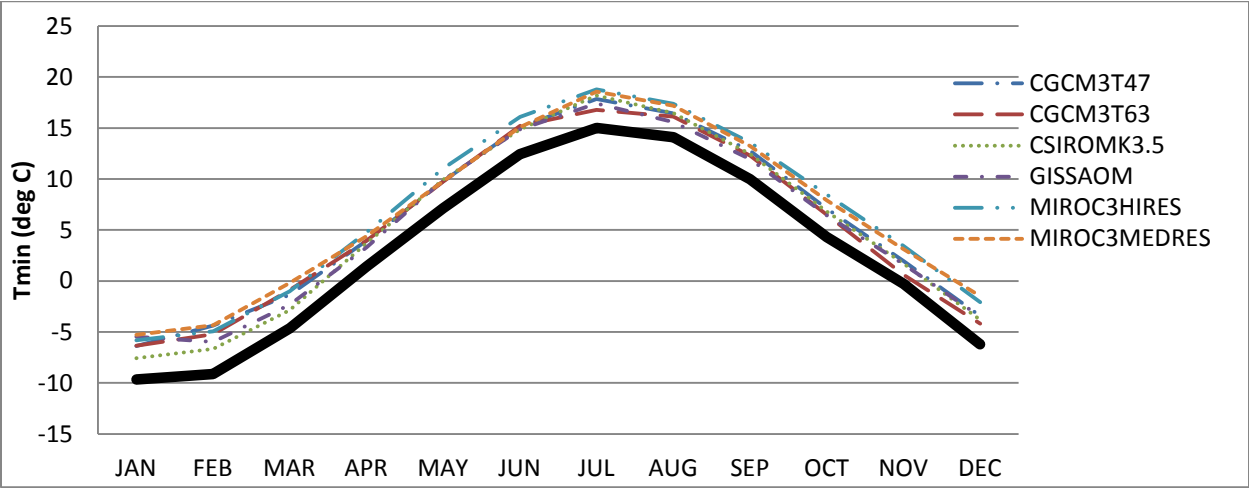
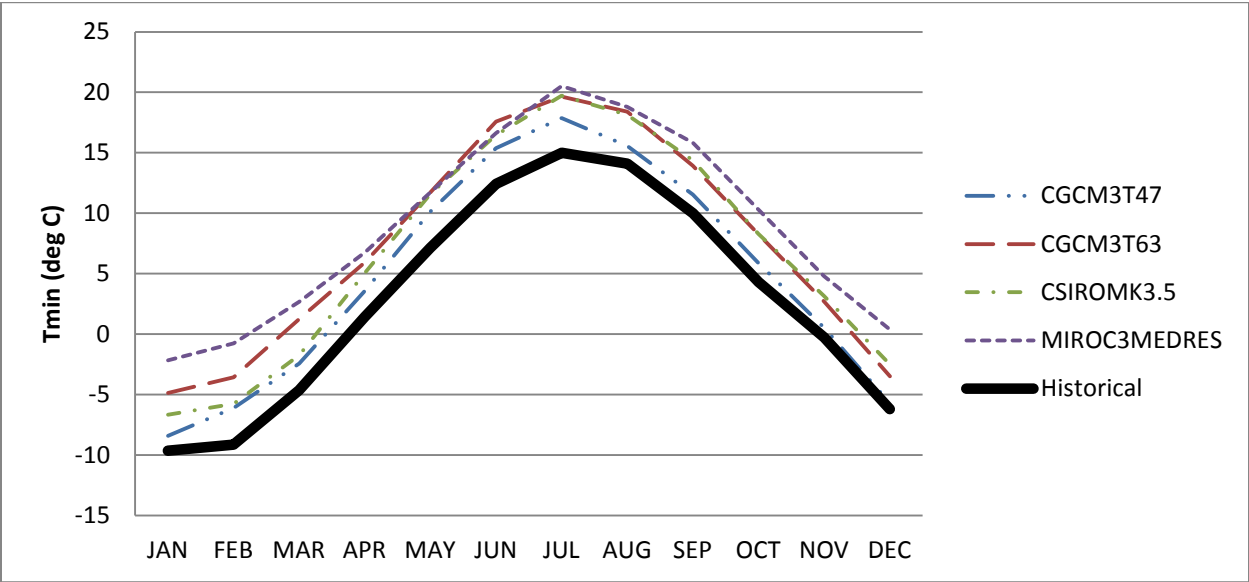


Figure 16: AOGCM predictions for minimum temperature, 2080s. Emission scenarios A1B, A2, B1 from top to bottom.

7. COMPARISON BETWEEN SDSM, LARS-WG, KnnCAD

To assess the performances of SDSM, LARS-WG, and KnnCAD simulated climate variables are compared to their equivalent historical values. Following a comparative performance evaluation, the downscaling models' abilities to simulate future daily precipitation is analysed and compared. Future precipitation amounts are studied as it is the most important variable in hydrologic modeling.

7.1 Comparative Performance Evaluation of LARS-WG, SDSM, KnnCAD

SDSM, LARS-WG, and KnnCAD results are presented in separate columns of **Figure 17**. The first row contains results for absolute minimum and maximum temperatures where the solid and dashed lines represent historical and simulated values, respectively. The goal of any downscaling model is to produce a strong agreement between the datasets so that ultimately the two lines will overlap. It is evident that KnnCAD reproduces temperature most accurately as the historical and simulated maximum temperature lines coincide and any discrepancy between values for minimum temperature is minor. LARS-WG produces reasonable temperature results as well. Historical and simulated values coincide for the months of January, March, April, May, July, and September. In addition, the difference in historical and simulated values from October to December is minimal. Simulation of minimum temperature is slightly less accurate as only results for January, June, September, and December agree, however the overall correlation is still quite strong. SDSM output captures the seasonal trend well but the historical range is significantly lower than the simulated range. Maximum temperature outputs only coincide in August and December, and there is no overlap in minimum temperature results.

Box plots are used to represent simulated total monthly precipitation results in the second row of **Figure 17**, with historical medians shown as a line plot. The historical median line is well within the inter-quartile range of simulated monthly precipitation amounts for all three models. There are some over or underestimations in total monthly precipitation values for certain months depending on the model. It is evident that LARS-WG and KnnCAD are most successful at reproducing total monthly precipitation amounts, particularly in the months of April, May, and December.

The third row of **Figure 17** shows the mean and standard deviation in daily precipitation by month, represented as a line plot. The top line shows the standard deviation while the bottom line shows daily mean precipitation. LARS-WG and KnnCAD produce far superior results than SDSM. SDSM's projection of mean daily precipitation is significantly underestimated between the months of June to September. Such results contradict the Dibike (2004) study in the Chute-du-Diable Basin in Quebec, where SDSM successfully reproduced the mean and standard deviation of daily precipitation.

Overall, LARS-WG and KnnCAD are found to be more capable of reproducing the observed climate. SDSM has shortcomings in the simulation of historical trends in daily precipitation and temperature. The results of this performance evaluation should be taken into account in the comparison of AOGCM downscaling results to understand the validity of the different future climate projections.

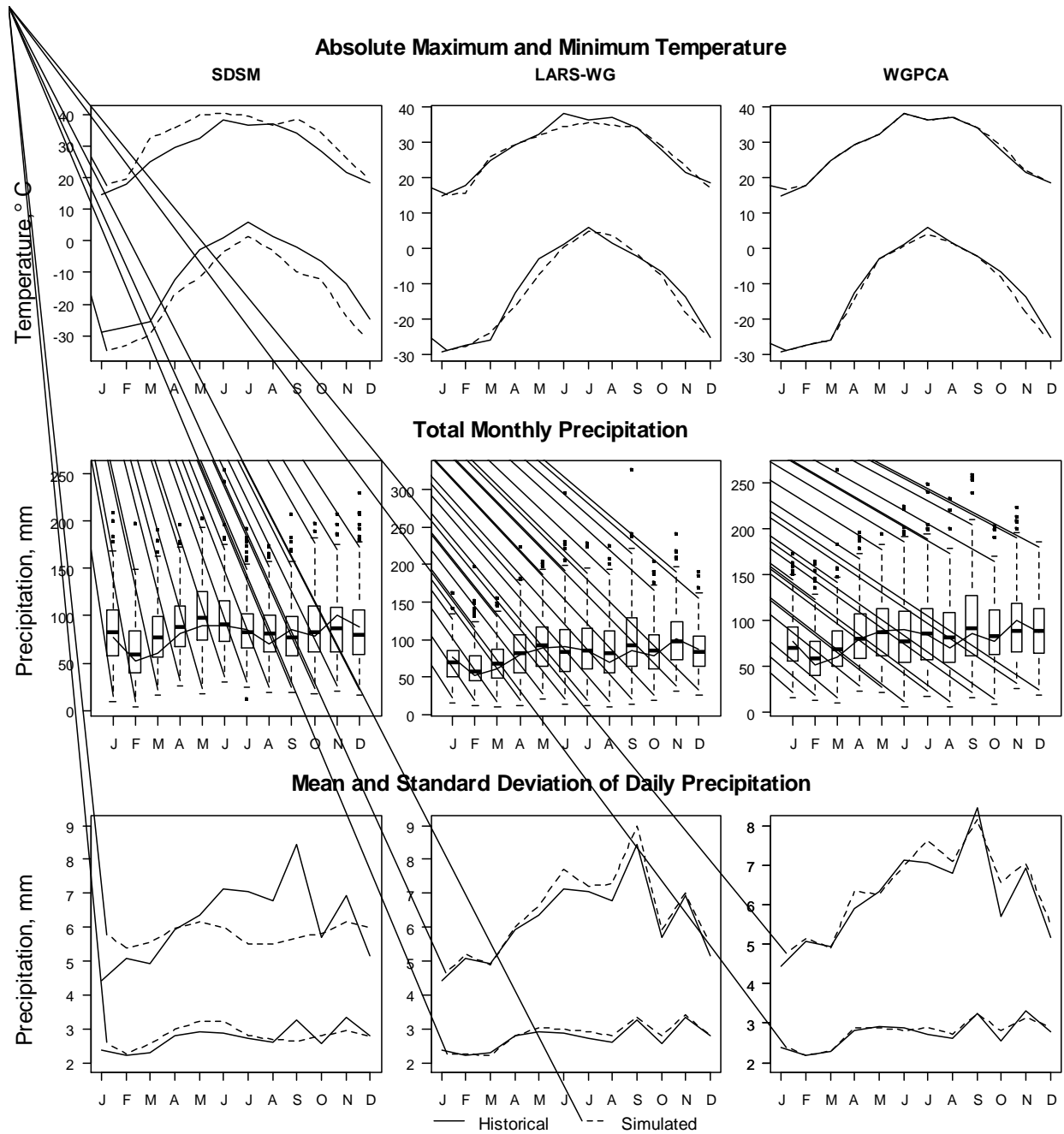


Figure 17: Comparative performance evaluation results for LARS-WG, SDSM, and KnnCAD

7.2 Comparative Generation of Future Daily PPT by LARS-WG, SDSM, KnnCAD

The comparative analysis of future precipitation amount is broken into four seasons as there are distinct trends within winter, spring, summer and fall months. Fifteen simulations are executed for the three stochastic downscaling models, each using different AOGCM output to perturb the historical input. Refer to **Table 2** for a list of AOGCMs and their available emissions scenarios.

Table 3 includes results for percent change in seasonal precipitation amounts between baseline and 2050 time periods. Positive values indicate an increase in total seasonal precipitation between time periods, alternatively negative results indicate a decrease in precipitation. Each simulation results in a 324-year time series of data, therefore 324 total seasonal precipitation results are averaged to obtain a single value representative of a downscaling model and AOGCM combination; i.e. SDSM with CGCM3T47 A1B output used to perturb the historical input

For the winter season SDSM tends to project the greatest average precipitation increases of 14.1%, 15.0%, and 17.8% for scenarios A1B, A2, and B1 respectively. The highest predicted increase for the winter season and A1B scenario is 20.8% projected by SDSM with MIROC3.2HIRES. All results are positive for the A1B scenario although the KnnCAD and LARS-WG models predict a smaller magnitude of increase overall. Such results indicate a strong agreement among the various models that winter precipitation amount will increase by the 2050s. When driven by scenario A2, SDSM projects the greatest precipitation increase of 26.5% using CGCM3T63 output. KnnCAD also produces significant positive results from CGCM3T47 at 24.8%. LARS-WG is the only model to predict decreases in winter precipitation, although the

magnitude of such decreases are low. Using MIROC3.2MEDRES output, LARS-WG projects decreases of 0.9% and 2.2% for scenarios A2 and B1, respectively, and another relatively insignificant decrease of 1.2% with GISSAOM B1.

The three stochastic models provide a mixture of results for the spring season. For the A1B scenario LARS-WG projects the highest average precipitation increase at 11.3%. KnnCAD provides similar output of 9.2%, and SDSM projects a much smaller increase of 1.9%. This low value is the result of a mixture of relatively significant positive and negative outcomes that have a cancelling effect on each other. CGCM3T47 and CGCM3T63 simulations project increases of 13.1% and 11.5%, respectively, while GISSAOM, MIROC3.2HIRES, and MIROC3.2MEDRES project decreases up to 8%. LARS-WG also projects a 6.0% decrease in precipitation using the MIROC3.2HIRES model output, while all other LARS-WG and KnnCAD results are positive for both A1B and A2 scenarios. Again, the average percent change predicted by SDSM for scenario A2 is relatively insignificant at 2.2%. For the same scenario, LARS-WG and KnnCAD project positive average results of 12.0% and 13.5%, respectively. The most significant positive percent change from scenario A2 is a 22.1% increase projected by KnnCAD, using the CGCM3T47 output. There are far more negative results in the spring season for the B1 scenario. SDSM projects the most significant decreases in spring precipitation ranging from 1.3% to 7.4%, with only one increase of 2.1% projected using the CGCM3T47 model. About half of LARS-WG simulations project an increase and the remainder project a decrease in spring precipitation. KnnCAD results are similar to LARS-WG in that two simulations predict decreases and the remaining four simulations predict increases of about 3.0% to 21.0%, resulting in a 13.5% average precipitation increase.

The downscaling models produce highly variable results for the summer season. SDSM, LARS-WG, and KnnCAD project average percent changes of 7.8%, -1.0%, and -7.2%, respectively from the A1B emissions scenario. The most significant decrease in precipitation is -17.8% projected by the KnnCAD, MIROC3.2MEDRES simulation. Conversely, the most significant increase in precipitation is 14.2% projected by the SDSM, GISSAOM simulation. The A2 scenario yields similar results to the A1B driven output. SDSM's averaged percent change is identical to that of the A1B scenario at 7.8%. For LARS-WG, the CSIRO Mk3.5 A2 simulation projects a 20.9% increase in precipitation which is the largest observed increase for the summer season. For the same downscaling tool CGCM3T47 and CGCM3T63 simulations project relatively insignificant changes of 1.2% and -1.2%, and the MIROC3.2HIRES simulation projects an 8.2% decrease in seasonal precipitation. All KnnCAD results range from about -4% to -16%, with the exception of the CSIRO Mk3.5 simulation which yields an increase of 10.1%. Increases in precipitation occur most frequently using the B1 scenario. All SDSM outputs are positive ranging from 4.2% to 13.0%, with an average percent change of 10.0%. LARS-WG results are more variable as CGCM3T47 and MIROC3.2HIRES simulations predict decreases of 2% and 6%, respectively. The remaining simulations predict increases up to 27%. The KnnCAD results are divided with some models projecting more precipitation and others projecting less precipitation. The outcomes range from a decrease of 15% to an increase of 22.5% for summer precipitation. Overall there was little agreement among downscaling tools and models on the sign, and magnitude of change for summer precipitation.

In the fall season, all A1B driven SDSM simulations agree that seasonal precipitation will decrease between 6% to 19%. Alternatively, LARS-WG simulations predict an increase ranging from about 3% to 42%. The 42% increase is the most extreme outcome for the A1B scenario,

projected by LARS-WG using the CGCM3T63 data to alter the historical input. The KnnCAD model also produced its highest output using this scenario, at 38.8%. KnnCAD results are generally similar to LARS-WG as most outcomes are positive ranging from around 7% to 39%, with the exception of one negative value of -4.7% projected using MIROC3.2MEDRES output. Results for the A2 and B1 scenarios follow a very similar pattern to the A1B scenario described above. Average results for scenario A2 are -13.4%, 14.9%, and 11.1% for SDSM, LARS-WG, and KnnCAD, respectively. Again, all SDSM simulations project negative results, while all LARS-WG and KnnCAD outcomes are positive with the exception of the MIROC3.2MEDRES simulations projecting decreases of around 4% each. As in the A1B scenario, the CGCM3T63 A2 simulations project the most extreme precipitation increases of 46% and 39% for LARS-WG and KnnCAD, respectively. Average changes predicted for the B1 scenario are -10.8%, 13.8%, and 9.1% for SDSM, LARS-WG, and KnnCAD, respectively. This time the MIROC3.2HIRES simulation produces a decrease in fall precipitation for LARS-WG and KnnCAD, and MIROC3.2MEDRES predicts a negative percent change for KnnCAD only. All other results for the two weather generators are positive, while SDSM projects decreases in precipitation ranging from around 4% to 23%. Once again, CGCM3T63 projects the most significant increases of around 55% and 42% for LARS-WG and KnnCAD.

Emission Scenario	AOGCM	Winter			Spring			Summer			Fall		
		SDSM	LARS-WG	KnnCAD	SDSM	LARS-WG	KnnCAD	SDSM	LARS-WG	KnnCAD	SDSM	LARS-WG	KnnCAD
A1B	CGCM3T47	10.5	16.5	18.7	13.1	20.5	17.6	-3.6	0.6	-3.9	-11.0	6.3	7.2
	CGCM3T63	13.7	13.0	13.2	11.5	15.8	10.1	4.7	-1.1	-5.1	-19.3	41.5	38.8
	GISSAOM	14.3	5.5	7.6	-7.0	13.1	4.7	14.2	13.1	7.0	-6.2	11.5	10.4
	MIROC3.2HIRES	20.8	18.4	16.2	-8.1	-6.0	1.0	11.1	-3.0	-16.0	-12.5	9.7	7.3
	MIROC3.2MEDRES	11.2	0.4	2.9	-0.1	12.9	12.6	12.7	-14.5	-17.8	-10.2	2.7	-4.7
Average A1B		14.1	10.8	11.7	1.9	11.3	9.2	7.8	-1.0	-7.2	-11.8	14.3	11.8
A2	CGCM3T47	18.1	21.7	24.8	4.0	15.0	22.1	6.2	1.2	-9.9	-17.2	10.6	6.6
	CGCM3T63	21.8	4.9	5.6	3.6	11.0	8.4	3.5	-1.2	-3.8	-17.8	46.2	39.4
	CSIRO MK3.5	7.4	9.8	13.5	0.1	15.2	14.1	10.2	20.9	10.1	-8.4	7.6	2.3
	MIROC3.2MEDRES	13.6	-0.9	2.5	1.4	7.5	13.5	11.2	-8.2	-15.5	-12.0	-4.1	-4.5
Average A2		15.0	9.2	11.6	2.2	12.0	13.5	7.8	2.3	-5.2	-13.4	14.9	11.1
B1	CGCM3T47	20.4	11.9	16.1	2.1	18.4	14.8	4.2	-2.4	-5.9	-15.4	6.3	6.0
	CGCM3T63	26.5	12.9	22.7	-1.3	-3.4	-4.5	5.3	11.9	5.8	-17.8	54.6	41.6
	CSIRO MK3.5	7.0	4.1	7.3	-7.1	16.1	13.7	13.0	27.4	22.5	-4.2	9.2	4.4
	GISSAOM	18.4	-1.2	8.4	-7.4	-0.5	-0.9	12.8	12.8	11.0	-7.9	6.2	6.6
	MIROC3.2HIRES	21.0	5.2	5.3	-5.1	-0.6	2.7	10.0	-5.9	-15.1	-14.2	-2.3	-3.6
	MIROC3.2MEDRES	16.1	-2.2	3.2	-5.8	23.0	20.7	8.9	1.2	-3.7	-9.6	1.1	-3.4
Average B1		17.8	3.8	9.4	-5.3	6.9	6.3	10.0	9.5	4.1	-10.8	13.8	9.1

Table 2: Percent change results for total seasonal precipitation amounts for SDSM, LAR-WG, and KnnCAD; 2050s

8. CONCLUSION

In this study a detailed analysis of LARS-WG is performed and its ability to produce historical and future output is compared with that of two other downscaling tools, namely SDSM and KnnCAD. The models are tested using input data from the London Airport station in the Upper Thames River Basin of Ontario Canada. Simulations of 324 years of historical climate data are produced to provide for a performance evaluation. Following this, 324-year simulations are produced for each of the 15 AOGCM scenarios in the 2020, 2050, and 2080 future time periods.

LARS-WG's ability to reproduce precipitation amount, precipitation frequency, and minimum and maximum temperatures is tested in a detailed performance evaluation. It is determined that total monthly precipitation, total monthly number of wet days, and minimum and maximum temperatures are simulated quite well. The parameters are slightly over or underestimated in certain months, however the historical median values are well within the inter-quartile ranges of the simulated data. LARS-WG simulates spell lengths relatively well despite an underestimation in the number of one-day wet spells and an overestimation in two-day spell occurrence. Overall, LARS-WG's performance in the preservation of historical statistics is deemed satisfactory.

A detailed analysis of LARS-WG's future climatic output includes total monthly precipitation, total monthly number of wet days, and minimum and maximum temperatures. Trends in total monthly precipitation are divided into three seasons. In the late winter and early spring, and the fall and early winter seasons the majority of AOGCMs project an increase in precipitation. Results are mixed in the late spring and early summer. The magnitudes of percent change are generally more significant in the 2080s indicating a greater amount of precipitation in

the first two seasons and a significantly drier late spring and summer season, especially in September. Results for total number of wet days vary considerably between months and exhibit little correlation between time periods, although within most months models are quite agreeable. All AOGCM scenarios project an increase in minimum and maximum temperatures except for one occurrence where the GISSAOM outcomes project higher average maximum temperatures in May than in June. This is likely due to an error in change factor application. Overall, there is a strong agreement among all models that temperatures will increase as a result of human induced climate change.

A comparative performance evaluation is carried out for SDSM, LARS-WG and KnnCAD prior to evaluation of the downscaling results. The models' abilities to reproduce absolute minimum and maximum temperatures, total monthly precipitation, and the mean and standard deviation of daily precipitation are tested. All models produce satisfactory results, with the exception of SDSM's output for the mean and standard deviation of daily precipitation values as there is great discrepancy between historical and simulated datasets.

The downscaling of 15 AOGCM models is performed using three different tools, and their outputs are compared. For the winter season, results show that SDSM projects the most significant increase in precipitation between time periods, while both LARS-WG and KnnCAD projections are less significant. The opposite is true for the spring season as LARS-WG and KnnCAD results are positive and generally of a greater magnitude than SDSM outcomes. Many SDSM simulations are negative or fairly similar to the historical climate. The trend in the model output changes again in the summer. SDSM consistently projects the most significant precipitation increase for scenarios A1B, A2, and B1. LARS-WG results vary considerably and most KnnCAD results predict decreases in precipitation. Finally in the fall, all SDSM results

predict precipitation decreases, while most LARS-WG and KnnCAD results predict precipitation increases of similar magnitudes. There is also a similarity between simulations that use CGCM3T63 output to perturb the historical datasets. Such results are far greater for both LARS-WG and KnnCAD models using all emissions scenarios in the fall season. Overall, there does not seem to be a relationship between SDSM and the other downscaling tools. This is likely due to the various statistical assumptions programmed in the models' structures. It is important to consider a variety of downscaling tools as well as a range of AOGCM models as each will produce different results even when the same model input is used. For a comprehensive climate change assessment, the assumption of a single downscaling tool or one AOGCM does not provide for an adequate range of potential events.

REFERENCES

- Apipattanavis, S., Podesta, G., Rajagopalan, P., Katz, R. W. (2007). "A semiparametric multivariate and multisite weather generator". *Water Resources Research* 43, W11401.
- Beersma, J. J., Buishand, T. A., Wojcik, R. (2001). "Rainfall generator for the Rhine Basin: multi-site simulation of daily weather variables by nearest-neighbour resampling". In: Generation of Hydro meteorological reference conditions for the assessment of flood hazard in large river basins, P. Krahe and D. Herpertz (Eds.), CHR-Report No. I-20, Lelystad, p. 69-77.
- Brandsma, T., Buishand, T. A., (1998). "Simulation of extreme precipitation in the Rhine basin by nearest-neighbour resampling". *Hydrology and Earth System Sciences* 2(2-3): 195-209.
- Brissette, F., Khalili, M., Leconte, R. (2007). "Efficient stochastic generation of multi-site synthetic precipitation data". *Journal of Hydrology* 345: 121-133.
- Brissette, F., Leconte, R., Minville, M., Roy, R. (2006). "Can we adequately quantify the increase/decrease of flooding due to climate change?". EIC Climate Change Technology Conference 2006, Ottawa, May 10-12. 1-6.
- Canadian Centre for Climate Modelling and Analysis (2010). "The Third Generation Coupled Global Climate Model". *Environment Canada*. Retrieved August 4, 2011 from <http://www.ec.gc.ca/ccmac-cccma/default.asp?lang=En&n=1299529F-1>
- Canadian Climate Change Scenarios Network (2010). "SRES scenarios background". *Environment Canada*. Retrieved August 5, 2010 from <http://ontario.cccsn.ca/?page=scen-sres>.
- CSIRO for the Department of Climate Change. (2009). "Hot Topics: How reliable are climate models?". *Australia Government Department of Climate Change*. Retrieved August 14,

2011from<http://www.climatechange.gov.au/climatechange/~media/publications/science/hot-topics-climate-models.ashx>

- Corte-Real, J., Xu, H., Qian, B. (1999). "A weather generator for obtaining daily precipitation scenarios based on circulation patterns". *Climate Research* 13: 61-75.
- Diaz-Neito, J., Wilby, R. L. (2005). "A comparison of statistical downscaling and climate change factor methods: Impacts on low flows in the River Thames, United Kingdom". *Climatic Change* 69: 245-268.
- Dibike, Y. B., Coulibaly, P. (2005). "Hydrologic impact of climate change in the Saguenay watershed: comparison of downscaling methods and hydrologic models". *Journal of Hydrology* 307: 144-163.
- Eum, H-I., Arunachalam V., Simonovic, S.P. (2009). "Integrated Reservoir Management System for Adaptation to Climate Change Impacts in the Upper Thames River Basin". *Water Resources Research Report 62*, Facility for Intelligent Decision Support, Department of Civil and Environmental Engineering, London, Ontario, Canada.
- Hanson, C. L., Johnson, G. L. (1998). "GEM (Generation of weather Elements for Multiple applications): its application in areas of complex terrain". *Hydrology, Water Resources and Ecology in Headwaters IAHS* 248: 27-32.
- IPCC, (2007). "Climate Change 2007: The Physical Science Basis. Contribution of Working Group I to the Fourth Assessment Report of the Intergovernmental Panel on Climate Change". Cambridge University Press, Cambridge, United Kingdom and New York, NY, USA, 996 pp.
- Khalili M., Brisette F., Leconte, R. (2008). "Stochastic multi-site generation of daily weather data". *Stoch Environ Res Risk Assess* (2009) 23: 837-849.

- Khan, M. S., Coulibaly, P., Dibike, Y. 2006. "Uncertainty analysis of statistical downscaling methods" *Journal of Hydrology* 319: 357-382.
- King, L., T.Solaiman and S. P. Simonovic (2009). "[Assessment of Climatic Vulnerability in the Upper Thames River Basin](#)". *Water Resources Research Report no. 064*, Facility for Intelligent Decision Support, Department of Civil and Environmental Engineering, London, Ontario, Canada, 62 pages. ISBN: (print) 978-0-7714-2816-6; (online) 978-0-7714-2817-3.
- King, L., T.Solaiman and S. P. Simonovic (2010). "[Assessment of Climatic Vulnerability in the Upper Thames River Basin: Part 2](#)". *Water Resources Research Report no. 066*, Facility for Intelligent Decision Support, Department of Civil and Environmental Engineering, London, Ontario, Canada, 72 pages. ISBN: (print) 978-0-7714-2834-0; (online) 978-0-7714-2835-7.
- Koukidis, E.N. and Berg, A.A. (2009). "Sensitivity of the Statistical Downscaling Model (SDSM) to reanalysis products. *Atmosphere-Ocean*, 47, 1-18.
- Kuchar, L. (2004). "Using WGENK to generate synthetic daily weather data for modelling of agricultural processes". *Mathematics and Computers in Simulation* 65: 69–75.
- LARS-WG 5: Quick Start (2010). "LARS-WG 5: a stochastic weather generator for climate change impact assessments". *Rothamsted Research*. Retrieved May 25, 2011 from <http://www.rothamsted.ac.uk/mas-models/download/LARSWG-QuickStart.pdf>
- Mason, S.J. (2004). "Simulating climate over western North America using stochastic weather generators". *Climate Change* 62: 155-187.
- NARR (2007). "North American Regional Reanalysis Homepage." *National Centres for Environmental Prediction (NCEP)*. Retrieved September 26, 2011 from <http://www.emc.ncep.noaa.gov/mmb/rrean/>

- PCMDI (2005). "Model Information of Potential Use to the IPCC Lead Authors and the AR4: GISS-AOM". *CMIP3 Climate Model Documentation, References, and Links*. Retrieved 23 Aug 2009 from http://www-pcmdi.llnl.gov/ipcc/model_documentation/GISS-AOM.htm.
- Prodanovic, P., Simonovic, S. P. (2007). "Development of rainfall intensity duration frequency curves for the City of London under the changing climate". *Water Resources Research Report* no. 58, Facility for Intelligent Decision Support, Department of Civil and Environmental Engineering, London, Ontario, Canada.
- Richardson, C.W. (1981). "Stochastic simulation of daily precipitation, temperature, and solar radiation". *Water Resources Research* 17: 182–90.
- Sarwar, R., Irwin, S., King, L., and S. P. Simonovic (2012). "[Assessment of Climatic Vulnerability in the Upper Thames River Basin: Downscaling with SDSM](#)". *Water Resources Research Report*, Facility for Intelligent Decision Support, Department of Civil and Environmental Engineering, London, Ontario, Canada
- Semenov, M. A., Barrow, E. M. (1997). "Use of a stochastic weather generator in the development of climate change scenarios". *Climatic Change* 35: 397-414.
- Semenov, M. A., Barrow, E. M. (2002). "LARS-WG: A stochastic weather generator for use in climate impact studies." *Rothamsted Research*. Retrieved May 15, 2011 from <http://www.rothamsted.ac.uk/mas-models/download/LARS-WG-Manual.pdf>
- Semenov M. A., Roger J. B. (1999). "Spatial interpolation of the LARS-WG stochastic weather generator in Great Britain". *Climate Research* 11: 137-148.
- Sharif, M., Burn, D. H., (2007). "Improved K-Nearest Neighbour weather generating model". *Journal of Hydrologic Engineering* 12: 42-51.
- Statistics Canada (a). *Hydrography – Lakes*. Ottawa; 2006.

- Statistics Canada (b). *Hydrography – Coast*. Ottawa; 2006.
- Soltani, A., Hoogenboom, G. (2003). “A statistical comparison of the stochastic weather generators WGEN and SIMMETEO”. *Climate Research* 24: 215-230.
- Thames Topics (1999). "Booklet 4: Floods". *Upper Thames River Conservation Authority*.
Retrieved August 4, from
http://www.thamesriver.on.ca/downloads/Thames_Topics/images/tt-book4.pdf
- Lee, K. (2010). *Daylight Hours Explorer*. University of Nebraska-Lincoln Astronomy Education.
<http://astro.unl.edu/classaction/animations/coordsmotion/daylighthousexplorer.html>
- Wilby, R.L. (2004). "Guidelines for Use of Climate Scenarios Development from Statistical Downscaling Methods."
- Wilby, R.L. and Dawson, C.W. (2007). "SDSM 4.2 - A decision support tool for the assessment of regional climate change impacts". *Department of Geography, Lancaster University, UK*.
Retrieved November 10, 2011 from
<http://copublic.lboro.ac.uk/cocwd/SDSM/SDSMManual.pdf>
- Wilks, D.S.(1998).“Multi-site generalization of a daily stochastic precipitation model”. *Journal of Hydrology* 210: 178–191.
- Zhang, X., Harvey, K., Hogg, W. and Yuzyk, T. (2001). “Trends in Canadian streamflow”.
Water Resources Research 37: 987-998.

APPENDIX A: AOGCM DATA DESCRIPTION

Coupled Global Climate Model: The third generation Coupled Global Climate Model (CGCM3) is an atmospheric-ocean model used in the IPCC's Fourth Assessment Report (2007) to produce extensive model simulations. It was developed by the Canadian Centre for Climate Modeling and Analysis (CCCma), which is a division of the Climate Research Branch of Environment Canada. The model runs at two resolutions, T47 and T63. The lower resolution model, CGCM3T47, has a grid size of 3.75° latitude by 3.75° longitude and 31 vertical layers. The CGCM3T63 model provides a slightly higher resolution of $2.8^\circ \times 2.8^\circ$ also with 31 vertical layers, (CCCma, 2010). Both versions are driven by A1B, A2, and B1 emissions scenarios which each provide potential, yet divergent, atmospheric greenhouse gas concentrations for the future.

Commonwealth Scientific and Industrial Research Organizations Mk3.5 Climate Systems

Model: Commonwealth Scientific and Industrial Research Organization (CSIRO) is located in Australia and is one of the largest and diverse scientific agencies in the world. The Marine and Atmospheric research division of CSIRO developed a coupled global climate model with atmosphere, land surface, ocean, polar ice components known as CSIRO Mk3.5. Its predecessor (CSIRO Mk3.0) appeared in the IPCC's Fourth Assessment Report and improvements were made to create CSIRO Mk3.5. Such improvements include reduced drift in the global mean temperature. CSIRO Mk 3.5 has a spatial resolution of $1.875^\circ \times 1.875^\circ$ with 18 vertical levels, (Collier, Dix, and Hirst, 2010). Emissions scenarios A2 and B1 are used as input as scenario A1B is not available for this AOGCM on the CCCSN database.

Goddard Institute for Space Studies Atmospheric Ocean Model: NASA's Goddard Institute for Space Studies (GISS) explores the global affects of natural and human induced change to our

environment on various time scales. In 2004 they released their own global climate model, GISS-AOM. It has a spatial resolution of 4° longitude and 3° latitude, 12 atmospheric layers, and up to 16 oceanic layers, (Atmosphere-Ocean Model, 2007). Emissions scenarios A1B and B1 are used to drive this model.

Model for Interdisciplinary Research on Climate 3.2: The Model for Interdisciplinary Research on Climate 3.2 (MIROC3.2) was developed at the Centre for Climate System Research at the University of Tokyo, National Institute for Environmental Studies, and the Frontier Research Centre. This model runs at two resolutions MIROC3.2HIRES and MIROC3.2MEDRES. MIROC3.2HIRES (high resolution) has a spatial resolution of 1.125° x 1.125° and is driven by emissions scenarios A1B and B1. MIROC3.2MEDRES (medium resolution) differs from MIROC3.2HIRES only in resolution as it has a coarser grid size of 2.8° x 2.8°, (PCMDI, 2005). All three emissions scenarios (A1B, A2, B1) are available and used as input to the MIROC3.2MEDRES version.

APPENDIX B: SRES EMISSIONS SCENARIOS

The IPCC's Special Report on Emissions Scenarios (SRES) contains scenarios with both greenhouse gas and sulphate aerosol forcings. In general, emissions scenarios provide input to the AOGCMs for evaluating climatic and environmental consequences of future greenhouse gas emissions, (IPCC, 2000). Greenhouse gases are considered positive forcings, and sulphate aerosols are negative forcings as they scatter and absorb solar radiation. Nevertheless, they negatively impact the environment by indirectly altering cloud properties and longevity.

Several divergent scenarios are used when simulating global climate data as recommended by the IPCC to ensure a wide range of future variables are considered in analysis, thus reducing uncertainty. The IPCC's Fourth Assessment Report (2007) uses three primary emission scenarios in their multi-model ensemble which include A1B, A2, and B1. All three scenarios are separately used as input to the AOGCMs for this study.

A1B: The SRES A1 storyline has three sub-categories that all describe a future with alternative development of energy technology. These sub-scenarios include A1FI, A1B, and A1T which represent fossil-fuel intensive, balanced, and predominantly non-fossil fuel technological advances, respectively. The A1B scenario was used in the IPCC's Fourth Assessment Report as well as in this study. It illustrates an integrated world of rapid economic and population growth on a global scale. The population peaks at approximately 9 billion mid-century and declines thereafter. New technologies consume a combination of clean non-fossil fuels and fossil fuels that are a major contributor to greenhouse gas emissions.

A2: The SRES A2 emissions scenario is similar to A1 as it portrays an economic future, but it is more heterogeneous. Countries are self-reliant and the feeling of nationalism is strong. As a result technological change and economic growth per capita is slower than in other storylines. It is understood that globalisation would increase these rates of growth.

B1: As in the A1 emissions scenario the SRES B1 scenario describes a world with a global population that peaks mid-century and declines after. As a result of globalisation, there have been rapid changes in economic structure. It is a positive outlook of a future with reduced material consumption and the introduction of clean, resource-efficient technologies.

APPENDIX C: 2050 RESULTS FOR LARS-WG

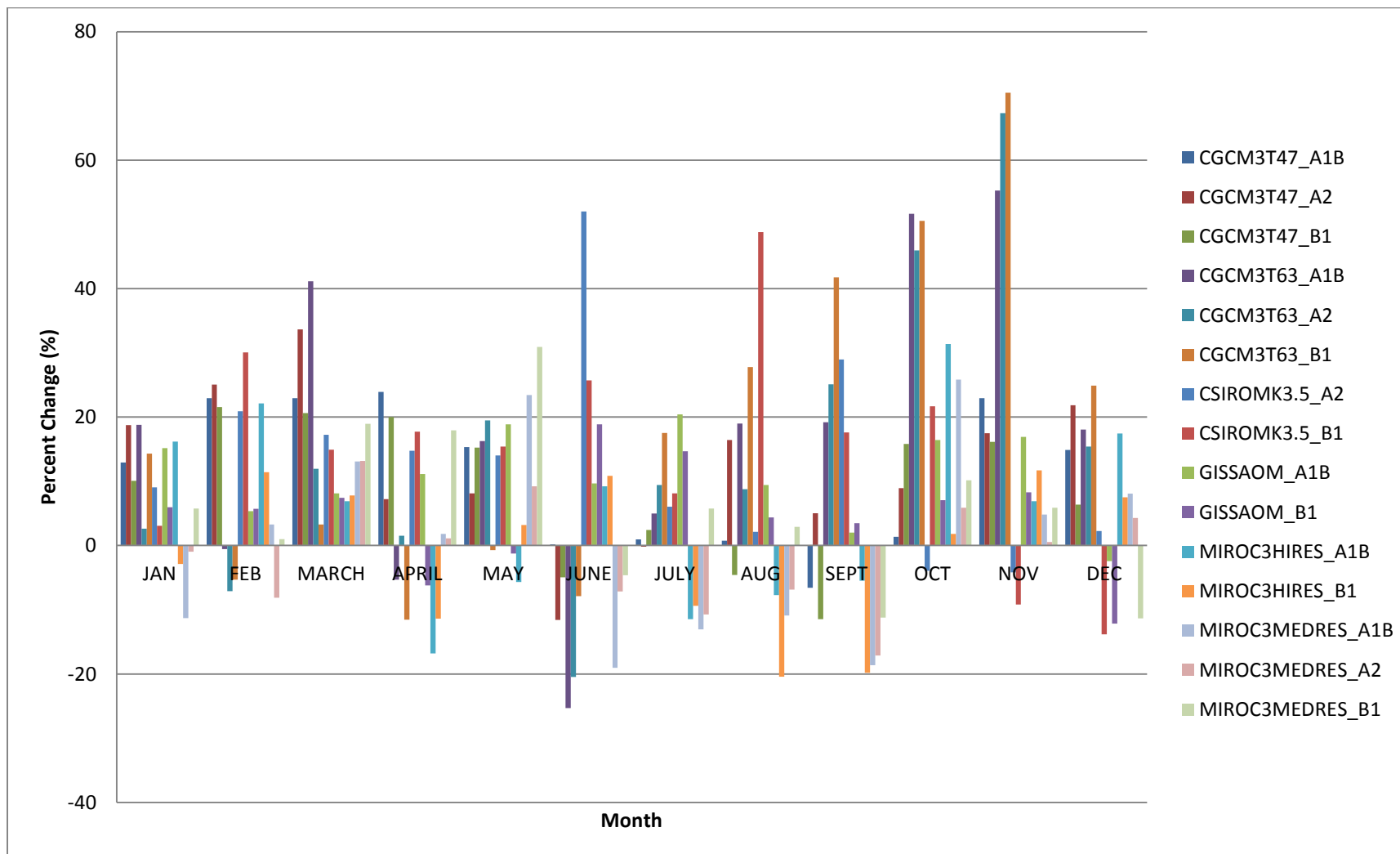


Figure 18: Percent change in total monthly precipitation, 2050s

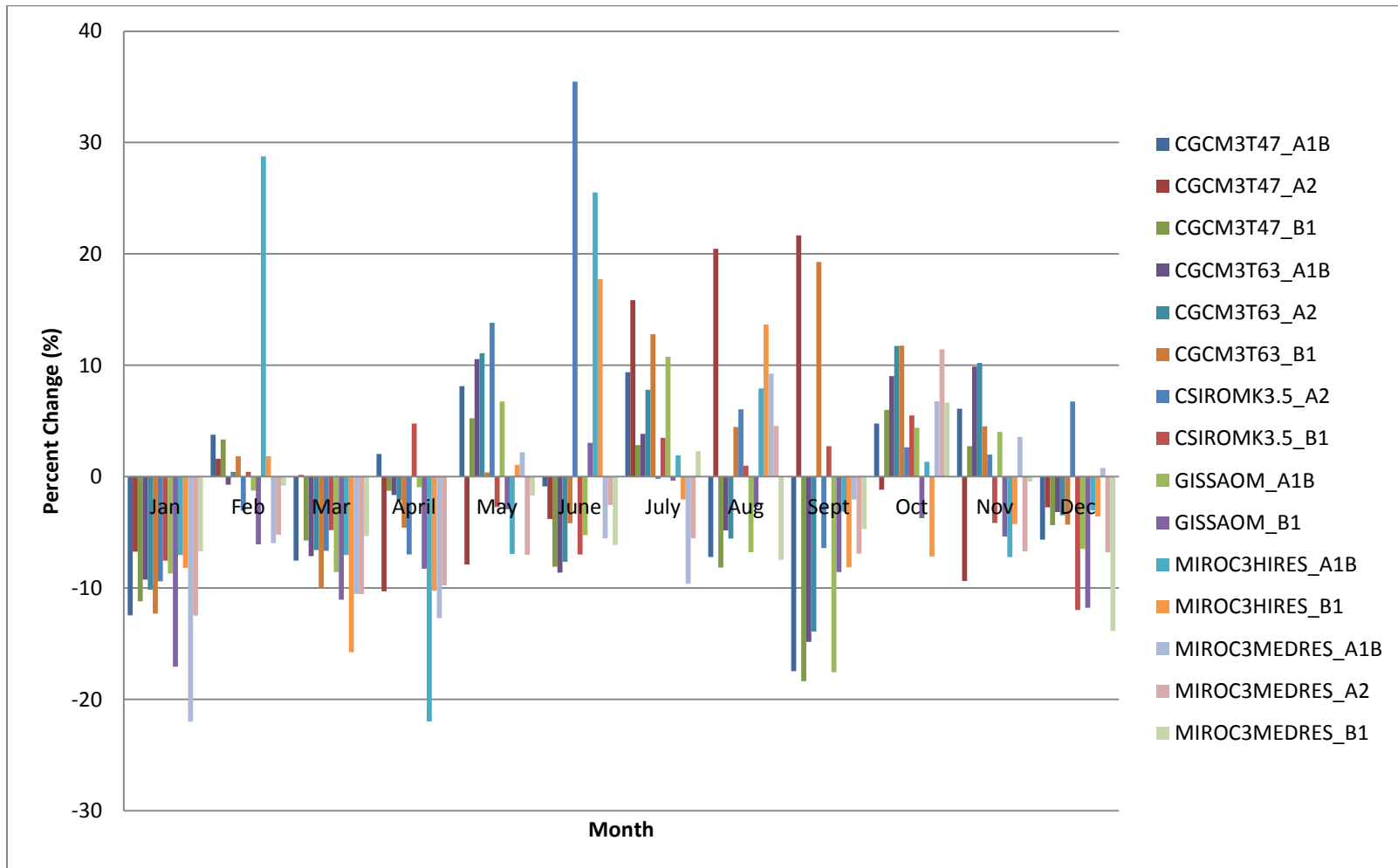


Figure 19: Percent change in total monthly number of wet days, 2050s

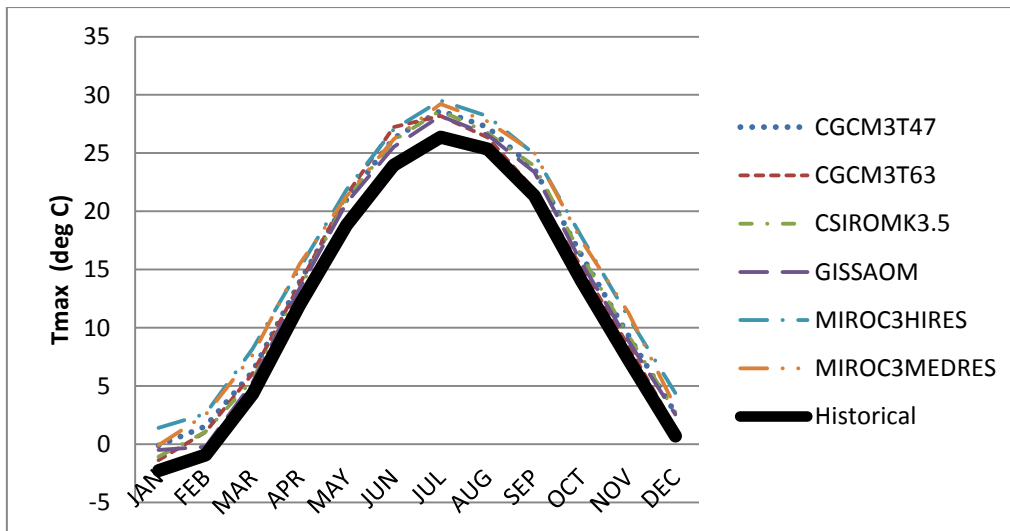
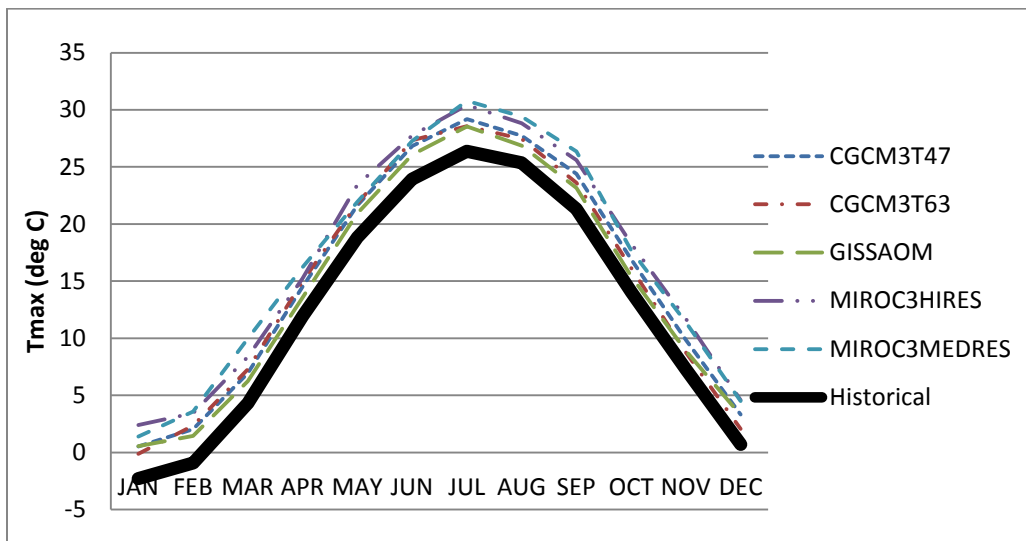
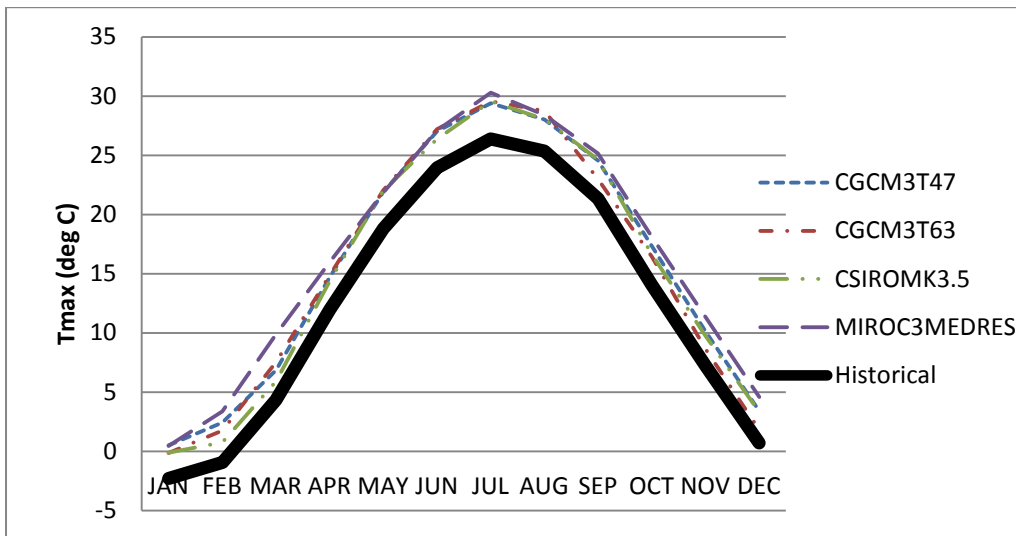


Figure 20: AOGCM predictions for maximum temperature, 2050s. Emission scenarios A1B, A2, B1 from top to bottom.

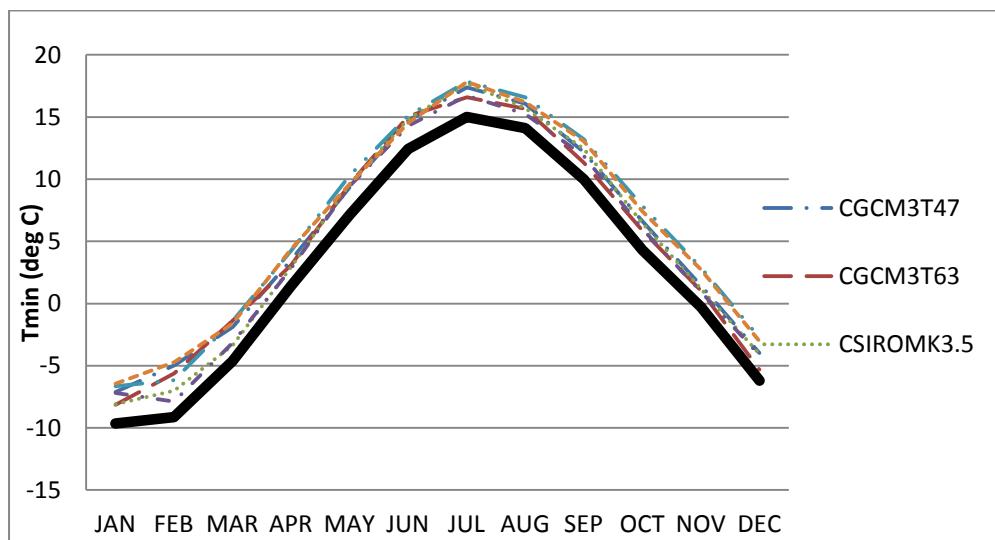
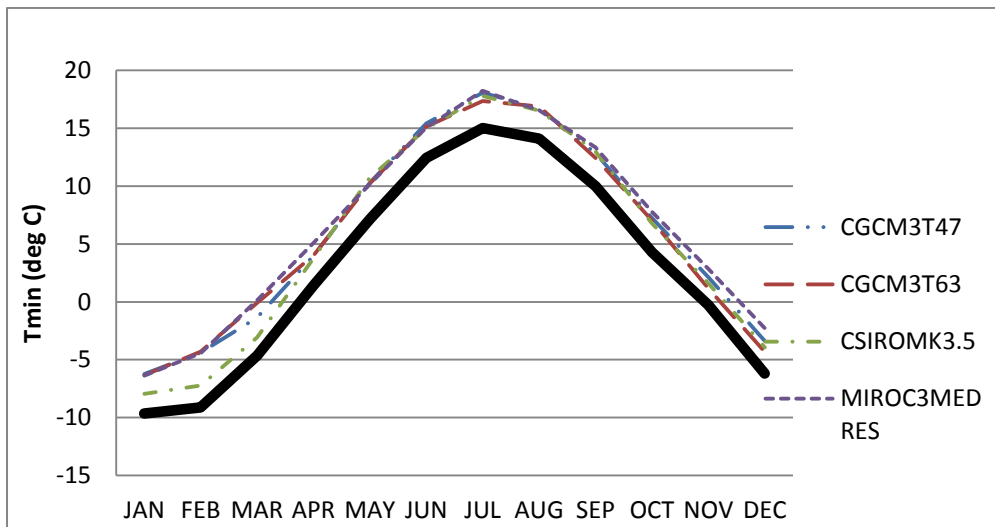
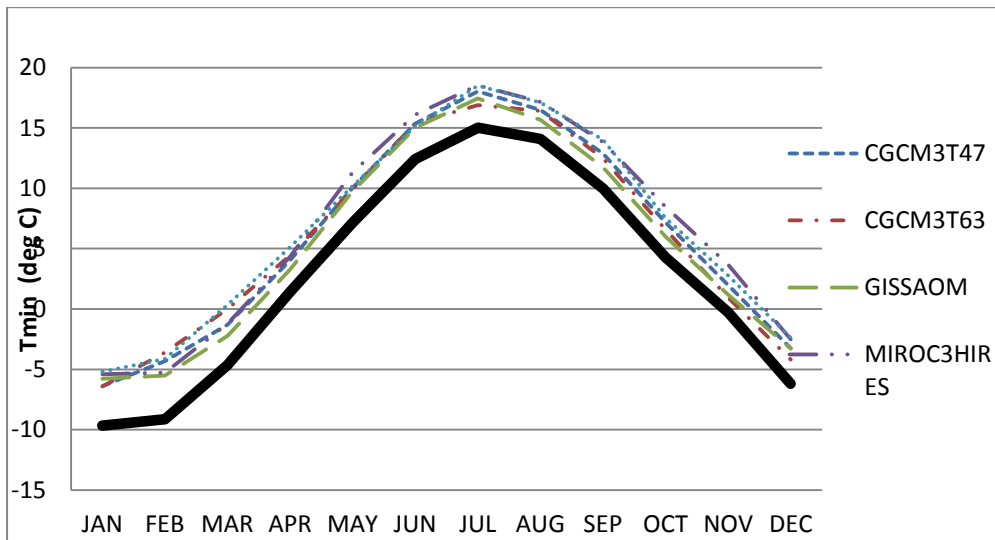


Figure 21: AOGCM predictions for minimum temperature, 2050s. Emission scenarios A1B, A2, B1 from top to bottom

APPENDIX D: PREVIOUS REPORTS IN THE SERIES

ISSN: (print) 1913-3200; (online) 1913-3219

(1) Slobodan P. Simonovic (2001). Assessment of the Impact of Climate Variability and Change on the Reliability, Resiliency and Vulnerability of Complex Flood Protection Systems. Water Resources Research Report no. 038, Facility for Intelligent Decision Support, Department of Civil and Environmental Engineering, London, Ontario, Canada, 91 pages. ISBN: (print) 978-0-7714-2606-3; (online) 978-0-7714-2607-0.

(2) Predrag Prodanovic (2001). Fuzzy Set Ranking Methods and Multiple Expert Decision Making. Water Resources Research Report no. 039, Facility for Intelligent Decision Support, Department of Civil and Environmental Engineering, London, Ontario, Canada, 68 pages. ISBN: (print) 978-0-7714-2608-7; (online) 978-0-7714-2609-4.

(3) Nirupama and Slobodan P. Simonovic (2002). Role of Remote Sensing in Disaster Management. Water Resources Research Report no. 040, Facility for Intelligent Decision Support, Department of Civil and Environmental Engineering, London, Ontario, Canada, 107 pages. ISBN: (print) 978-0-7714-2610-0; (online) 978-0-7714-2611-7.

(4) Taslima Akter and Slobodan P. Simonovic (2002). A General Overview of Multiobjective Multiple-Participant Decision Making for Flood Management. Water Resources Research Report no. 041, Facility for Intelligent Decision Support, Department of Civil and Environmental Engineering, London, Ontario, Canada, 65 pages. ISBN: (print) 978-0-7714-2612-4; (online) 978-0-7714-2613-1.

(5) Nirupama and Slobodan P. Simonovic (2002). A Spatial Fuzzy Compromise Approach for Flood Disaster Management. Water Resources Research Report no. 042, Facility for Intelligent Decision Support, Department of Civil and Environmental Engineering, London, Ontario, Canada, 138 pages. ISBN: (print) 978-0-7714-2614-8; (online) 978-0-7714-2615-5.

(6) K. D. W. Nandalal and Slobodan P. Simonovic (2002). State-of-the-Art Report on Systems Analysis Methods for Resolution of Conflicts in Water Resources Management. Water Resources Research Report no. 043, Facility for Intelligent Decision Support, Department of Civil and Environmental Engineering, London, Ontario, Canada, 216 pages. ISBN: (print) 978-0-7714-2616-2; (online) 978-0-7714-2617-9.

(7) K. D. W. Nandalal and Slobodan P. Simonovic (2003). Conflict Resolution Support System – A Software for the Resolution of Conflicts in Water Resource Management. Water Resources Research Report no. 044, Facility for Intelligent Decision Support, Department of Civil and Environmental Engineering, London, Ontario, Canada, 144 pages. ISBN: (print) 978-0-7714-2618-6; (online) 978-0-7714-2619-3.

(8) Ibrahim El-Baroudy and Slobodan P. Simonovic (2003). New Fuzzy Performance Indices for Reliability Analysis of Water Supply Systems. Water Resources Research Report no. 045, Facility for Intelligent Decision

Support, Department of Civil and Environmental Engineering, London, Ontario, Canada, 90 pages. ISBN: (print) 978-0-7714-2620-9; (online) 978-0-7714- 2621-6.

(9) Juraj Cunderlik (2003). Hydrologic Model Selection for the CFCAS Project: Assessment of Water Resources Risk and Vulnerability to Changing Climatic Conditions. Water Resources Research Report no. 046, Facility for Intelligent Decision Support, Department of Civil and Environmental Engineering, London, Ontario, Canada, 40 pages. ISBN: (print) 978-0-7714- 2622-3; (online) 978-0-7714- 2623-0.

(10) Juraj Cunderlik and Slobodan P. Simonovic (2004). Selection of Calibration and Verification Data for the HEC-HMS Hydrologic Model. Water Resources Research Report no. 047, Facility for Intelligent Decision Support, Department of Civil and Environmental Engineering, London, Ontario, Canada, 29 pages. ISBN: (print) 978-0-7714-2624-7; (online) 978-0-7714-2625-4.

(11) Juraj Cunderlik and Slobodan P. Simonovic (2004). Calibration, Verification and Sensitivity Analysis of the HEC-HMS Hydrologic Model. Water Resources Research Report no. 048, Facility for Intelligent Decision Support, Department of Civil and Environmental Engineering, London, Ontario, Canada, 113 pages. ISBN: (print) 978- 0-7714-2626-1; (online) 978-0-7714- 2627-8.

(12) Predrag Prodanovic and Slobodan P. Simonovic (2004). Generation of Synthetic Design Storms for the Upper Thames River basin. Water Resources Research Report no. 049, Facility for Intelligent Decision Support, Department of Civil and Environmental Engineering, London, Ontario, Canada, 20 pages. ISBN: (print) 978- 0-7714-2628-5; (online) 978-0-7714-2629-2.

(13) Ibrahim El-Baroudy and Slobodan P. Simonovic (2005). Application of the Fuzzy Performance Indices to the City of London Water Supply System. Water Resources Research Report no. 050, Facility for Intelligent Decision Support, Department of Civil and Environmental Engineering, London, Ontario, Canada, 137 pages. ISBN: (print) 978-0-7714-2630-8; (online) 978-0-7714-2631-5.

(14) Ibrahim El-Baroudy and Slobodan P. Simonovic (2006). A Decision Support System for Integrated Risk Management. Water Resources Research Report no. 051, Facility for Intelligent Decision Support, Department of Civil and Environmental Engineering, London, Ontario, Canada, 146 pages. ISBN: (print) 978-0-7714-2632-2; (online) 978-0-7714-2633-9.

(15) Predrag Prodanovic and Slobodan P. Simonovic (2006). Inverse Flood Risk Modelling of The Upper Thames River Basin. Water Resources Research Report no. 052, Facility for Intelligent Decision Support, Department of Civil and Environmental Engineering, London, Ontario, Canada, 163 pages. ISBN: (print) 978-0-7714-2634-6; (online) 978-0-7714-2635-3.

(16) Predrag Prodanovic and Slobodan P. Simonovic (2006). Inverse Drought Risk Modelling of The Upper Thames River Basin. Water Resources Research Report no. 053, Facility for Intelligent Decision Support, Department of Civil and Environmental Engineering, London, Ontario, Canada, 252 pages. ISBN: (print) 978-0-7714-2636-0; (online) 978-0-7714-2637-7.

(17) Predrag Prodanovic and Slobodan P. Simonovic (2007). Dynamic Feedback Coupling of Continuous Hydrologic and Socio-Economic Model Components of the Upper Thames River Basin. Water Resources Research Report no. 054, Facility for Intelligent Decision Support, Department of Civil and Environmental Engineering, London, Ontario, Canada, 437 pages. ISBN: (print) 978-0-7714-2638-4; (online) 978-0-7714-2639-1.

(18) Subhankar Karmakar and Slobodan P. Simonovic (2007). Flood Frequency Analysis Using Copula with Mixed Marginal Distributions. Water Resources Research Report no. 055, Facility for Intelligent Decision Support, Department of Civil and Environmental Engineering, London, Ontario, Canada, 144 pages. ISBN: (print) 978-0-7714-2658-2; (online) 978-0-7714-2659-9.

(19) Jordan Black, Subhankar Karmakar and Slobodan P. Simonovic (2007). A Web-Based Flood Information System. Water Resources Research Report no. 056, Facility for Intelligent Decision Support, Department of Civil and Environmental Engineering, London, Ontario, Canada, 133 pages. ISBN: (print) 978-0-7714-2660-5; (online) 978-0-7714-2661-2.

(20) Angela Peck, Subhankar Karmakar and Slobodan P. Simonovic (2007). Physical, Economical, Infrastructural and Social Flood Risk – Vulnerability Analyses in GIS. Water Resources Research Report no. 057, Facility for Intelligent Decision Support, Department of Civil and Environmental Engineering, London, Ontario, Canada, 80 pages. ISBN: (print) 978-0-7714-2662-9; (online) 978-0-7714-2663-6.

(21) Predrag Prodanovic and Slobodan P. Simonovic (2007). Development of Rainfall Intensity Duration Frequency Curves for the City of London Under the Changing Climate. Water Resources Research Report no. 058, Facility for Intelligent Decision Support, Department of Civil and Environmental Engineering, London, Ontario, Canada, 51 pages. ISBN: (print) 978-0-7714-2667-4; (online) 978-0-7714-2668-1.

(22) Evan G. R. Davies and Slobodan P. Simonovic (2008). An integrated system dynamics model for analyzing behaviour of the social-economic-climatic system: Model description and model use guide. Water Resources Research Report no. 059, Facility for Intelligent Decision Support, Department of Civil and Environmental Engineering, London, Ontario, Canada, 233 pages. ISBN: (print) 978-0-7714-2679-7; (online) 978-0-7714-2680-3.

(23) Vasan Arunachalam (2008). Optimization Using Differential Evolution. Water Resources Research Report no. 060, Facility for Intelligent Decision Support, Department of Civil and Environmental Engineering, London, Ontario, Canada, 42 pages. ISBN: (print) 978-0-7714-2689-6; (online) 978-0-7714-2690-2.

(24) Rajesh Shrestha and Slobodan P. Simonovic (2009). A Fuzzy Set Theory Based Methodology for Analysis of Uncertainties in Stage-Discharge Measurements and Rating Curve. Water Resources Research Report no. 061, Facility for Intelligent Decision Support, Department of Civil and Environmental Engineering, London, Ontario, Canada, 104 pages. ISBN: (print) 978-0-7714-2707-7; (online) 978-0-7714-2708-4.

- (25) Hyung-II Eum, Vasan Arunachalam and Slobodan P. Simonovic (2009). Integrated Reservoir Management System for Adaptation to Climate Change Impacts in the Upper Thames River Basin. Water Resources Research Report no. 062, Facility for Intelligent Decision Support, Department of Civil and Environmental Engineering, London, Ontario, Canada, 81 pages. ISBN: (print) 978-0-7714-2710-7; (online) 978-0-7714-2711-4.
- (26) Evan G. R. Davies and Slobodan P. Simonovic (2009). Energy Sector for the Integrated System Dynamics Model for Analyzing Behaviour of the Social- Economic-Climatic Model. Water Resources Research Report no. 063. Facility for Intelligent Decision Support, Department of Civil and Environmental Engineering, London, Ontario, Canada. 191 pages. ISBN: (print) 978-0-7714-2712-1; (online) 978-0-7714-2713-8.
- (27) Leanna King, Tarana Solaiman, and Slobodan P. Simonovic (2009). Assessment of Climatic Vulnerability in the Upper Thames River Basin. Water Resources Research Report no. 064, Facility for Intelligent Decision Support, Department of Civil and Environmental Engineering, London, Ontario, Canada, 61pages. ISBN: (print) 978-0-7714-2816-6; (online) 978-0-7714- 2817-3.
- (28) Slobodan P. Simonovic and Angela Peck (2009). Updated Rainfall Intensity Duration Frequency Curves for the City of London under Changing Climate. Water Resources Research Report no. 065, Facility for Intelligent Decision Support, Department of Civil and Environmental Engineering, London, Ontario, Canada, 64pages. ISBN: (print) 978-0-7714-2819-7; (online) 987-0-7714-2820-3.
- (29) Leanna King, Tarana Solaiman, and Slobodan P. Simonovic (2010). Assessment of Climatic Vulnerability in the Upper Thames River Basin: Part 2. Water Resources Research Report no. 066, Facility for Intelligent Decision Support, Department of Civil and Environmental Engineering, London, Ontario, Canada, 72pages. ISBN: (print) 978-0-7714-2834-0; (online) 978-0-7714-2835-7.
- (30) Christopher J. Popovich, Slobodan P. Simonovic and Gordon A. McBean (2010). Use of an Integrated System Dynamics Model for Analyzing Behaviour of the Social-Economic-Climatic System in Policy Development. Water Resources Research Report no. 067, Facility for Intelligent Decision Support, Department of Civil and Environmental Engineering, London, Ontario, Canada, 37 pages. ISBN: (print) 978-0-7714-2838-8; (online) 978-0-7714-2839-5.
- (31) Hyung-II Eum and Slobodan P. Simonovic (2009). City of London: Vulnerability of Infrastructure to Climate Change; Background Report 1 – Climate and Hydrologic Modeling. Water Resources Research Report no. 068, Facility for Intelligent Decision Support, Department of Civil and Environmental Engineering, London, Ontario, Canada, 102pages. ISBN: (print) 978-0-7714-2844-9; (online) 978-0-7714-2845-6.
- (32) Dragan Sredojevic and Slobodan P. Simonovic (2009). City of London: Vulnerability of Infrastructure to Climate Change; Background Report 2 – Hydraulic Modeling and Floodplain Mapping. Water Resources Research Report no. 069, Facility for Intelligent Decision Support, Department of Civil and Environmental Engineering, London, Ontario, Canada, 147 pages. ISBN: (print) 978-0-7714-2846-3; (online) 978-0-7714-2847-0.

(33) Tarana A. Solaiman and Slobodan P. Simonovic (2011). Quantifying Uncertainties in the Modelled Estimates of Extreme Precipitation Events at the Upper Thames River Basin. Water Resources Research Report no. 070, Facility for Intelligent Decision Support, Department of Civil and Environmental Engineering, London, Ontario, Canada, 167 pages. ISBN: (print) 978-0-7714-2878-4; (online) 978-0-7714-2880-7.

(34) Tarana A. Solaiman and Slobodan P. Simonovic (2011). Assessment of Global and Regional Reanalyses Data for Hydro-Climatic Impact Studies in the Upper Thames River Basin. Water Resources Research Report no. 071, Facility for Intelligent Decision Support, Department of Civil and Environmental Engineering, London, Ontario, Canada, 74 pages. ISBN: (print) 978-0-7714-2892-0; (online) 978-0-7714-2899-9.

(35) Tarana A. Solaiman and Slobodan P. Simonovic (2011). Development of Probability Based Intensity-Duration-Frequency Curves under Climate Change. Water Resources Research Report no. 072, Facility for Intelligent Decision Support, Department of Civil and Environmental Engineering, London, Ontario, Canada, 89 pages. ISBN: (print) 978-0-7714-2893-7; (online) 978-0-7714-2900-2.

(36) Dejan Vucetic and Slobodan P. Simonovic (2011). Water Resources Decision Making Under Uncertainty. Water Resources Research Report no. 073, Facility for Intelligent Decision Support, Department of Civil and Environmental Engineering, London, Ontario, Canada, 143 pages. ISBN: (print) 978-0-7714-2894-4; (online) 978-0-7714-2901-9.

(37) Angela Peck, Elisabeth Bowering and Slobodan P. Simonovic (2010). City of London: Vulnerability of Infrastructure to Climate Change, Final Report - Risk Assessment. Water Resources Research Report no. 074, Facility for Intelligent Decision Support, Department of Civil and Environmental Engineering, London, Ontario, Canada, 66 pages. ISBN: (print) 978-0-7714-2895-1; (online) 978-0-7714-2902-6.

(38) Akhtar, M. K., S. P. Simonovic, J. Wibe, J. MacGee, and J. Davies, (2011). An integrated system dynamics model for analyzing behaviour of the social-energy-economic-climatic system: model description. Water Resources Research Report no. 075, Facility for Intelligent Decision Support, Department of Civil and Environmental Engineering, London, Ontario, Canada, 211 pages. ISBN: (print) 978-0-7714-2896-8; (online) 978-0-7714-2903-3.

(39) Akhtar, M. K., S. P. Simonovic, J. Wibe, J. MacGee, and J. Davies, (2011). An integrated system dynamics model for analyzing behaviour of the social-energy-economic-climatic system: user's manual. Water Resources Research Report no. 076, Facility for Intelligent Decision Support, Department of Civil and Environmental Engineering, London, Ontario, Canada, 161 pages. ISBN: (print) 978-0-7714-2897-5; (online) 978-0-7714-2904-0.

(40) Millington, N., S. Das and S. P. Simonovic (2011). The Comparison of GEV, Log-Pearson Type 3 and Gumbel Distributions in the Upper Thames River Watershed under Global Climate Models. Water Resources Research Report no. 077, Facility for Intelligent Decision Support, Department of Civil and Environmental Engineering, London, Ontario, Canada, 53 pages. ISBN: (print) 978-0-7714-2898-2; (online) 978-0-7714-2905-7.

(41) Andre Schardong and Slobodan P. Simonovic (2012). Multi-objective Evolutionary Algorithms for Water Resources Management. Water Resources Research Report no. 078, Facility for Intelligent Decision Support,

Department of Civil and Environmental Engineering, London, Ontario, Canada, 167 pages. ISBN: (print) 978-0-7714-2907-1; (online) 978-0-7714-2908-8.

(42) Samiran Das and Slobodan P. Simonovic (2012). Assessment of Uncertainty in Flood Flows under Climate Change: the Upper Thames River basin (Ontario, Canada). Water Resources Research Report no. 079, Facility for Intelligent Decision Support, Department of Civil and Environmental Engineering, London, Ontario, Canada, 67 pages. ISBN: (print) 978-0-7714-2960-6; (online) 978-0-7714-2961-3.

(43) Rubaiya Sarwar, Sarah E. Irwin, Leanna M. King and Slobodan P. Simonovic (2012). Assessment of Climatic Vulnerability in the Upper Thames River basin: Downscaling with SDSM. Water Resources Research Report no. 080, Facility for Intelligent Decision Support, Department of Civil and Environmental Engineering, London, Ontario, Canada, 65 pages. ISBN: (print) 978-0-7714-2962-0; (online) 978-0-7714-2963-7.